MOLECULAR AND CELLULAR BIOLOGY, Sept. 1996, p. 5194–5209 Vol. 16, No. 9
0270-7306/96/$04.00+0

Sst2, a Negative Regulator of Pheromone Signaling in the Yeast *Saccharomyces cerevisiae*: Expression, Localization, and Genetic Interaction and Physical Association with Gpa1 (the G-Protein α Subunit)

HENRIK G. DOHLMAN,[1,2] JIANPING SONG,[1] DOREEN MA,[2]† WILLIAM E. COURCHESNE,[2]‡ AND JEREMY THORNER[2]*

Department of Pharmacology, Boyer Center for Molecular Medicine, Yale University School of Medicine, New Haven, Connecticut 06536-0812,[1] and Department of Molecular and Cell Biology, Division of Biochemistry and Molecular Biology, University of California, Berkeley, California 94720-3202

Received 3 May 1996/Returned for modification 6 June 1996/Accepted 24 June 1996

Sst2 is the prototype for the newly recognized RGS (for regulators of G-protein signaling) family. Cells lacking the pheromone-inducible *SST2* gene product fail to resume growth after exposure to pheromone. Conversely, overproduction of Sst2 markedly enhanced the rate of recovery from pheromone-induced arrest in the long-term halo bioassay and detectably dampened signaling in a short-term assay of pheromone response (phosphorylation of Ste4, Gβ subunit). When the *GPA1* gene product (Gα subunit) is absent, the pheromone response pathway is constitutively active and, consequently, growth ceases. Despite sustained induction of Sst2 (observed with specific anti-Sst2 antibodies), *gpa1*Δ mutants remain growth arrested, indicating that the action of Sst2 requires the presence of Gpa1. The N-terminal domain (residues 3 to 307) of Sst2 (698 residues) has sequence similarity to the catalytic regions of bovine GTPase-activating protein and human neurofibromatosis tumor suppressor protein; segments in the C-terminal domain of Sst2 (between residues 417 and 685) are homologous to other RGS proteins. Both the N- and C-terminal domains were required for Sst2 function in vivo. Consistent with a role for Sst2 in binding to and affecting the activity of Gpa1, the majority of Sst2 was membrane associated and colocalized with Gpa1 at the plasma membrane, as judged by sucrose density gradient fractionation. Moreover, from cell extracts, Sst2 could be isolated in a complex with Gpa1 (expressed as a glutathione *S*-transferase fusion); this association withstood the detergent and salt conditions required for extraction of these proteins from cell membranes. Also, *SST2*$^+$ cells expressing a GTPase-defective *GPA1* mutant displayed an increased sensitivity to pheromone, whereas *sst2* cells did not. These results demonstrate that Sst2 and Gpa1 interact physically and suggest that Sst2 is a direct negative regulator of Gpa1.

The yeast *Saccharomyces cerevisiae* is a useful organism in which to study hormone signaling (for reviews, see references 5, 94, and 100). The two haploid cell types (*MAT***a** and *MAT*α) each secrete a peptide pheromone (**a**-factor and α-factor, respectively) that acts on the other cell type to promote mating, resulting in the formation of a *MAT***a**/*MAT*α diploid cell. The **a** and α mating factors bind to cell surface receptors of the seven-transmembrane-segment class (for a review, see reference 34). The receptors are coupled to downstream events through direct activation of a heterotrimeric guanine nucleotide-binding protein (G protein) (for reviews, see references 14, 16, and 57). In response to receptor occupancy by pheromone, the G-protein α subunit (*GPA1* gene product) replaces bound GDP with GTP (13) and dissociates from the G-protein βγ complex (composed of the *STE4* and *STE18* gene products) (112, 114, 115). As long as Gα binds GTP, Gβγ is free to positively activate the subsequent response effectors, which include a cascade of protein kinases whose actions result in the induction of gene transcription, stimulation of morphological changes, and imposition of a G_1-specific block to cell cycle progression (for reviews, see references 46, 63, and 79). Upon GTP hydrolysis, Gα blocks further signaling via its reassociation with Gβγ (10, 26, 31, 75).

A universal feature of all signaling pathways in biological systems is the attenuation of the response upon prolonged exposure to an extracellular stimulus. The molecular basis for this desensitization or adaptation phenomenon is complex. In animal cells, desensitization is achieved via a variety of negative-feedback loops that interdict the signaling machinery at almost every level (for reviews, see references 64 and 73). In yeast cells, desensitization clearly occurs after exposure of a haploid cell to mating pheromone (77) and also involves multiple feedback events. For example, α-factor is degraded (24) by an extracellular protease encoded by a pheromone-inducible and *MAT***a** cell-specific gene (*BAR1*/*SST1*) (65, 66). The cytosolic tail of the α-factor receptor (*STE2* gene product) is phosphorylated in a pheromone-dependent manner (11, 86), and the receptor is cleared from the cell surface by pheromone-induced endocytosis (92, 105). In addition, Gβ (Ste4) becomes phosphorylated in a pheromone-dependent manner (25). Transcription of the Gα gene (*GPA1*) is stimulated by pheromone (49), but transcription of the Gβ (*STE4*) and Gγ (*STE18*) genes is not (44), and the proportion of newly made Gα that is *N*-myristoylated (33), a modification that is essential

* Corresponding author. Mailing address: Department of Molecular and Cell Biology, Division of Biochemistry and Molecular Biology, University of California, Room 401, Barker Hall, Corner of Hearst and Oxford Sts., Berkeley, CA 94720-3202. Phone: (510) 642-2558. Fax: (510) 643-5035.

† Present address: Lilly Research Laboratories, Eli Lilly and Company, Indianapolis, IN 46285.

‡ Present address: Department of Microbiology, University of Nevada, Reno, NV 89557.

for efficient coupling of Gα to the Gβγ complex (98, 102), is increased. As the result of these and other processes, yeast cells that fail to mate eventually resume normal growth and cell division, despite the extensive physiological and morphological changes that they have undergone in preparation for mating. Genetic analysis suggests, however, that additional gene products are also required. In particular, defects in the *SST2* locus (21, 22) cause a much more profound debility in desensitization than do mutations in any other gene yet identified (20, 86), indicating that Sst2 plays a critical role in adaptation and recovery. Nonetheless, the molecular basis of Sst2 function has remained unclear.

It has been reported (67) that overexpression of a ubiquitin-conjugating enzyme increases the turnover of Gpa1, resulting in a lower steady-state level of Gα and an arrest of cell growth. The observed growth inhibition was relieved by an *sst2*Δ mutation. On this basis, it was proposed that the function of Sst2 is to promote Gpa1 degradation. This model cannot be correct, however, because cells lacking Sst2 are hypersensitive to pheromone action and deficient in adaptation (22, 30, 86) whereas cells with elevated Gpa1 are less sensitive to pheromone than wild-type cells and recover faster (26, 31, 78, 113). In fact, the *GPA1* gene acts as a dosage suppressor of the pheromone hypersensitivity of *sst2* mutations (31, 75). Indeed, other studies have found no detectable effect of *sst2*Δ mutations on *GPA1* expression or Gpa1 turnover (32).

Previous observations are more consistent with a role for Sst2 in down-regulating the activity of the Gα subunit. Dominant mutations in *GPA1* that potentiate the resumption of growth following pheromone-induced arrest have been isolated (58, 74, 103). At least one of these alleles, $GPA1^{G50V}$, can manifest its phenotype in a strain carrying the *sst2-1* missense mutation (74) but not in a strain carrying an *sst2*Δ mutation (58). The fact that certain *GPA1* mutations can bypass the need for fully active *SST2* suggests that Sst2 may act directly on Gpa1 to control its functional state. Likewise, mutations in the *STE5* gene that activate the pathway downstream of Gβγ (but upstream of its other known components) grow poorly; this phenotype is exacerbated in *sst2* mutants and relieved in *sst2 ste4* cells, again consistent with the notion that Sst2 acts as a negative regulator somewhere between the receptor and Gα (45). Finally, dominant mutations in *SST2* that block pheromone response have been isolated (32). These mutations confer a pheromone-resistant phenotype but do not prevent activation of the pathway by overexpression of Gβ, by a mutation ($STE4^{Hpl}$) that constitutively activates Gβ, or by disruption of *GPA1*, indicating that Sst2 operates at a step coincident with (or upstream of) the Gα subunit.

To address the function of Sst2, we first reexamined its sequence. In addition to being the founding member of the newly emerging RGS (for regulators of G-protein signaling) family (for reviews, see references 88 and 96), we found other sequence features in Sst2 that bear on its potential physiological role and delineated the functional domains of Sst2 by mutational analysis. We also developed reagents to examine the level of expression, localization, and other biochemical properties of Sst2, including its ability to associate physically with Gpa1. Finally, we generated novel mutations in *GPA1* and examined their genetic interaction with *sst2* mutations. Our findings indicate that Gpa1 is the direct target of Sst2 action.

MATERIALS AND METHODS

Strains, media, and DNA-mediated transformation. *S. cerevisiae* strains used in this study are listed in Table 1. *Escherichia coli* HB101 was used for the propagation and maintenance of plasmids. Established methods were used for the growth and genetic manipulation of both *S. cerevisiae* (41, 95) and bacteria (3, 90). Liquid cultures and agar plates for the propagation of yeast contained either a rich medium (YPGlc) (95) or a synthetic medium (95) supplemented with appropriate nutrients to permit growth and maintain selection for plasmids, with 2% glucose (SCGlc) or 2% galactose and 0.2% sucrose (SCGal) as the carbon source. DNA-mediated transformation was carried out by the lithium acetate procedure (48).

TABLE 1. *S. cerevisiae* strains used in this study

Strain	Genotype	Source or reference
BC159	*MAT***a** *ade2-1^{oc} his3-Δ1 leu2-3,112 ura3-52*	28
BC180[a]	BC159 *sst2-Δ2*	This study
DJ803-11-1[b]	*MAT***a** *bar1-1 can1 cry1 cyh2 his4^{am} leu2 lys2^{oc} SUP4-3(am)^{ts} trp1^{am} ura3 ste5-3^{ts} GPA1^{+}*	D. D. Jenness
DJ803-2-1[b]	*MAT***a** *bar1-1 can1 cry1 cyh2 his4^{am} leu2 lys2^{oc} SUP4-3(am)^{ts} trp1^{am} ura3 ade2^{oc} ste5-3^{ts} gpa1::lacZ[LEU]*	D. D. Jenness
BJ2168	*MAT***a** *gal2 leu2 trp1 ura3-52 pep4-3 prb1-1122 prc1-407*	50
FC180	*MAT***a**/*MAT***a** *bar1/bar1 can1/can1 cry1/cry1 cyh2/+ his4^{am}/+ hmlα::LEU2/hmlα::LEU2 leu2/leu2 lys2^{oc}/lys2^{oc} SUP4-3(am)^{ts}/SUP4-3(am)^{ts} trp1^{am}/+ ura3/ura3*	F. R. Cross
RK512-5B	*MAT***a** *ade2-1^{oc} his3-Δ1 ura3-52 sst2-1*	28

[a] Strain BC159 was transformed with plasmid pBC14 (see Materials and Methods), which carries the *sst2-Δ2* deletion mutation, that had been cut at its unique *Nhe*I site. This site resides within the *SST2* sequences remaining in this deletion construct and targets integration of the plasmid into the chromosomal *SST2* locus. The resulting Ura^{+} transformants were then plated on plates containing 5-fluoroorotic acid (15) to select for derivatives in which the plasmid had been excised by a recombination event that left the *sst2-Δ2* allele behind in the chromosome in place of the normal gene (93). One such *ura3 sst2-Δ2* derivative was designated BC180.

[b] This is a set of congenic spores derived from an extensive series of backcrosses (9, 10) of strain 381G-42E (*ste5-3^{ts}*) with its parental strain, 381G (43). One of these strains was then transformed with a DNA construct containing the *gpa1::lacZ*[*LEU2*] allele (also called *scg1::lacZ*[*LEU2*]), which was kindly provided by J. Kurjan, Department of Microbiology and Molecular Genetics, University of Vermont, Burlington.

Plasmid construction. Restriction enzymes and buffers, T4 DNA polymerase, T4 DNA ligase, and calf intestinal phosphatase were obtained from Boehringer Mannheim or New England BioLabs. Standard cloning vectors used in this study were pUC19 (120) and pBluescript (Stratagene). pBS-HE was constructed by digestion of pBluescript with *Hin*dIII and *Eco*RI, converting the termini so generated to flush ends, and religating to yield a vector lacking *Hin*dIII and *Eco*RI sites. Yeast expression plasmids used in this study were pAB23 (which carries the *TDH3* promoter and terminator on an Amp^{R}- and *URA3*-marked, 2μm DNA-containing multicopy vector) (37), pAD4M (which carries the *ADH1* promoter and terminator on an Amp^{R}- and *LEU2*-marked, 2μm DNA-containing multicopy vector) (71), and YEp351 (an Amp^{R}- and *LEU2*-marked, 2-μm DNA-containing multicopy vector) (47).

***SST2* plasmids.** A 4.6-kb *Hin*dIII fragment containing the *SST2* gene (from nucleotide −940 to +2260, where +1 is the A of the ATG initiator codon) (27, 30) was inserted into the *Hin*dIII site of pUC19 to yield pUC19-*SST2*. The same *Hin*dIII fragment was inserted into the corresponding site in YEp351 to yield YEp351-*SST2*. The same *Hin*dIII fragment was ligated into the *Hin*dIII site in YIp5 (104), and then an internal *Hpa*I-*Hpa*I fragment was excised, which removed the promoter and 85% of the *SST2* coding sequence, yielding plasmid pBC14. To produce a TrpE-Sst2 fusion protein, a 2.1-kb *Sca*I-*Hin*dIII fragment (containing 1,096 bp of the C-terminal portion of the *SST2* open reading frame) was inserted immediately downstream of and in frame with the *E. coli trpE* gene in vector pATH22 (54) that had been digested with the same enzymes. A modified version of the *SST2* gene containing a *Bam*HI site at nucleotide −30 was prepared by oligonucleotide-directed mutagenesis (see below), and a *Bam*HI-*Hin*dIII fragment of this construction (from nucleotide −30 to +2260 of the *SST2* coding sequence) was converted to the flush-end form by treatment with T4 DNA polymerase and ligated into pAB23 that had been digested with *Bgl*II and converted to the blunt-end form by the same kind of treatment, yielding pAB23-*SST2*. C-terminal truncation alleles (*SST2Δ687*, *sst2Δ557*, and *sst2Δ253*), from which had been removed the last 11, 141, and 445 codons, respectively, of the *SST2* coding sequence, were constructed by ligation of a termination linker, consisting of two annealed, phosphorylated oligonucleotides

(5′-TAATAGGTAATAGGTAATAG-3′ and 5′-GATCCTATTACCTATTAC CTATTA-3′) that contained multiple stop codons in all three reading frames and a 4-bp overhang at one end, onto linearized pUC19-*SST2* that had been cleaved, respectively, at the *Nhe*I, *Sac*II, and *Cla*I sites in the *SST2* sequence and converted to the flush-end form. For expression in yeast cells, appropriate *Bam*HI-to-linker fragments of the resulting constructs were inserted into the *Bgl*II site in pAB23, yielding pAB23-SST2Δ687, pAB23-sst2Δ557, and pAB23-sst2Δ253, respectively. To construct N-terminal truncation alleles, DNA fragments were amplified by PCR using the normal *SST2* gene as the template, a common downstream primer (containing the *Bst*XI site at codon 199 of the *SST2* coding sequence), and three different upstream primers (5′-CCGTCGACTATCTGA GGCGTTATAG-3′, 5′-CCGTCGACAATGAGTGACACTAAGTCTTTC-3′, and 5′-CCGTCGACAATGGACAGAACTCGTGGCGAG-3′), each containing an artificial *Sal*I site, which generated products containing an initiator codon situated at codons 1, 55, and 125, respectively. The resulting products were substituted as *Sal*I-*Bst*XI fragments for the corresponding *Sal*I-*Bst*XI segment in full-length *SST2* that had been inserted into pBluescript. For expression in yeast cells, *Sal*I-*Eco*RI fragments from the resulting pBluescript constructs were inserted into pAD4M that had been digested with *Sal*I and *Eco*RI, yielding pAD4M-S/SST2(1–698), pAD4M-S/SST2(56–698), and pAD4M-S/SST2(126–698). All constructions were confirmed by direct nucleotide sequence determination. Functional expression of *SST2* from all of the yeast expression vectors constructed was confirmed either by a halo bioassay (see below), to assess the ability of the plasmid to complement the *sst2-Δ2* mutation in strain BC180, or by immunoblotting (see below), to detect the corresponding polypeptide.

***GPA1* plasmids.** A 1.7-kb *Xba*I fragment containing the *GPA1* gene (−93 to +1560 relative to the ATG initiator) was excised from pG1501 (75), converted to the blunt-end form, and ligated with pAB23 that had been digested with *Bgl*II and converted to the flush-end form, generating pAB23-*GPA1*. The same fragment was inserted into pBS-HE that had been cleaved with *Xba*I, yielding pBS-HE-*GPA1*. For expression in yeast cells, the *Sma*I-*Sac*I fragment containing the entire *GPA1* gene was excised from pBS-HE-*GPA1* and ligated into pAD4M that had been digested with the same enzymes. Vectors to express glutathione *S*-transferase (GST) alone and a *GPA1*-GST fusion in yeast cells were constructed as described in detail elsewhere (98). Functional expression of *GPA1* from all of the yeast expression vectors constructed was confirmed by the ability of the plasmid to complement the cold-sensitive lethality of strain DJ803-2-1 (*ste5^{ts} gpa1*Δ) or by immunoblotting (see below) to detect the corresponding polypeptide.

Site-directed mutagenesis. All synthetic oligonucleotides were prepared by staff of the Microchemical Facility of the Cancer Research Laboratory of the University of California at Berkeley. Successful introduction of the desired base substitutions and epitope tags, as well as preservation of the correct orientation and reading frame in all subsequent constructions, was verified by direct nucleotide sequence analysis (91).

Two different mutants of the *GPA1* gene product (with a substitution of L for Q at position 323 [Q323L] and a substitution of H for R at position 297 [R297H]) were constructed by inserting *GPA1* into the replicative form of bacteriophage M13 and using appropriate synthetic oligonucleotide primers (encoding the appropriate base substitutions to create both the desired codon change and a silent mutation that produced a unique restriction endonuclease cleavage site for diagnostic purposes) with the aid of a commercial kit (Amersham) for oligonucleotide-directed mutagenesis, in accordance with the manufacturer's instructions. Appropriate DNA fragments containing the *GPA1^{R297H}* and *GPA1^{Q323L}* alleles were inserted into the vector pAD4M as described above, thereby generating pAD4M-*GPA1^{R297H}* and pAD4M-*GPA1^{Q323L}*, respectively. An epitope-tagged version of the *GPA1* gene product that is recognized by the mouse anti-c-Myc monoclonal antibody (MAb) 9E10 (36) was constructed and inserted into pAB23, yielding pAB23-*GPA1*-myc, as described in detail elsewhere (98).

A version of the *SST2* gene containing a *Bam*HI site immediately preceding nucleotide −30 (where +1 is the A of the ATG of the *SST2* coding sequence) was constructed by using M13 mutagenesis and an appropriate oligonucleotide essentially as described immediately above. A version of the *SST2* gene product encoding a C-terminal c-Myc epitope tag was constructed in three steps. First, a double-stranded, blunt-ended synthetic oligonucleotide (5′-CTCGAGGAGCA GAAATTAATCAGCGAAGAGGACCTCCTCAGGAAGAGGTAA-3′ plus its complement) that encodes the amino acid sequence AEEQKLISEEDLL RKR-stop, which is also recognized by MAb 9E10, was ligated into the vector pBluescript that had been digested with *Eco*RV, yielding pBluescript-myc. Second, an *Eco*RI-*Nhe*I fragment containing *SST2* was excised from pAB23-*SST2*, converted to the flush-end form by treatment with T4 DNA polymerase, and ligated immediately upstream of and in frame with the epitope in pBluescript-myc that had been digested with *Xho*I, converted to the blunt-end form, and dephosphorylated by treatment with calf intestinal phosphatase, yielding pBS-*SST2*-myc. Third, a 3.1-kb *Bam*HI fragment containing the *SST2-myc* fusion, excised from pBS-*SST2*-myc, was inserted into the *Bgl*II site of pAB23, yielding pAB23-*SST2*-myc.

Preparation of anti-Sst2 antibodies and other antisera. To induce expression of the TrpE-Sst2 fusion protein, a culture (1 liter) of *E. coli* CAG512 carrying plasmid pATH22-*SST2* was grown at 30°C in M9 medium containing ampicillin and Casamino Acids (which lacks tryptophan) for 14 h. The cells were collected by centrifugation, washed by resuspension and recentrifugation in 100 ml of TEN (50 mM Tris-HCl [pH 7.5], 0.5 mM EDTA, 300 mM NaCl), resuspended in 50 ml of TEN containing 1 mg of lysozyme per ml, 0.2% Triton X-100, and 2 mg of pancreatic DNAse I per ml, and lysed by incubation on ice for 1 h. The lysate was subjected to centrifugation at 4,000 × *g* for 15 min. The resulting pellet (inclusion body fraction) was washed three times in 10 ml of TEN, resuspended in 12.5 ml of solubilization buffer (100 mM Tris-HCl [pH 7.5], 4 M urea, 10% glycerol, 0.1% sodium dodecyl sulfate [SDS], 2-mercaptoethanol), and incubated at 37°C for 30 min. The solubilized material was clarified by centrifugation at 4,000 × *g* for 15 min, and proteins in the supernatant solution were resolved by preparative-scale polyacrylamide gel electrophoresis (PAGE) in the presence of SDS. After staining with Coomassie brilliant blue, the 63-kDa TrpE-Sst2 fusion protein, which was the most prominent species present, was harvested electrophoretically in a commercial device (Elutrap; Schleicher & Schuell) according to the manufacturer's instructions. Samples of the electrophoretically purified fusion protein were used for immunization of adult female New Zealand White rabbits by standard procedures (42).

Preparation and characterization of rabbit polyclonal anti-Gpa1 antibodies have been described previously (33). The anti-c-Myc MAb was isolated as ascites fluid from nude mice injected with the 9E10-producing hybridoma cell line (36) (generously provided by J. M. Bishop, University of California at San Francisco), which were maintained by staff of the Hybridoma Facility of the Cancer Research Laboratory of the University of California at Berkeley. Affinity-purified rabbit polyclonal anti-Ste4 antibodies (25) were generously provided by G. Cole and S. I. Reed, Scripps Research Institute, La Jolla, Calif. Rabbit anti-GST antibodies were the gift of J. Steitz, Department of Molecular Biophysics and Biochemistry, Yale University School of Medicine, New Haven, Conn.

For monitoring subcellular fractionation, well-characterized affinity-purified antibodies directed against protein markers diagnostic for various cellular compartments were used. These antibodies, and descriptions of the proteins against which they were made, are as follows: anti-phosphoglycerate kinase (Pgk1), a cytosolic enzyme (6); anti-Sec61, an integral membrane protein of the endoplasmic reticulum (101); anti-α-factor receptor (Ste2), an integral membrane protein of the plasma membrane (12, 55); anti-Kex2, an integral membrane enzyme in a late compartment of the Golgi body (38, 85); anti-β subunit of the F_1-ATPase (Atp2), a peripheral membrane protein of the mitochondrial inner membrane (23); and anti-Sec4, a prenylated peripheral membrane protein associated with secretory vesicles and the plasma membrane (39).

Preparation of cell extracts. Yeast cultures were grown at 30°C for various time periods either in YPGlc or in selective medium (SCGlc) (when maintenance of plasmids was required), treated with various concentrations (0.5 to 5 μM) of synthetic α-factor (Peninsula Laboratories; stored as a 1-mg/ml stock solution in high-performance liquid chromatography [HPLC]-grade H_2O at −20°C) in the presence or absence of 10 μg of cycloheximide (Sigma) per ml (stored as a 1,000× stock solution in ethanol at −80°C). When *BAR1$^+$* cells were incubated with α-factor for longer than 1 h, 25 mM sodium succinate (pH 3.5) was added to the medium to inhibit α-factor proteolysis (24). To terminate growth, NaN_3 was added to a final concentration of 10 mM and the cultures were immediately chilled on ice. The cells were collected by centrifugation at 4°C, washed by resuspension and recentrifugation in ice-cold 10 mM NaN_3, and resuspended in ice-cold lysis buffer A (100 mM Tris-HCl [pH 7.4], 10 mM EDTA, 1 mM dithiothreitol, 0.1 mM phenylmethylsulfonyl fluoride). Cell density was determined on the basis of the A_{600}, and equivalent numbers of cells of each sample were transferred to 1.5-ml Eppendorf tubes and pelleted by brief centrifugation. The resulting pellets were then homogenized in one of two ways. To prepare extracts for subsequent subcellular fractionation, the resuspended cells were ruptured by four 1-min pulses of vigorous vortex mixing with an approximately equal volume of glass beads (0.45- to 0.50-mm diameter) alternating with 1-min periods of cooling on ice. The lysate was cleared of unbroken cells and large debris by centrifugation at 450 × *g* for 20 min. The resulting supernatant solution was subjected to centrifugation for 20 min at 100,000 × *g* in the TLA 100.3 rotor of a tabletop ultracentrifuge (Beckman model TL100). The resulting supernatant solution and pellet fraction were each resuspended in an equal volume of SDS-PAGE sample buffer (50 mM Tris-HCl [pH 6.8], 1% SDS, 1% 2-mercaptoethanol, 10% glycerol, 0.003% bromophenol blue) (60) and solubilized by boiling for 10 min. To prepare whole-cell extracts, the washed cells were resuspended directly in SDS-PAGE sample buffer, dissolved by boiling for 10 min, subjected to homogenization by four 1-min pulses of vigorous vortex mixing with glass beads at room temperature, and clarified by brief centrifugation in a microcentrifuge.

Gel electrophoresis and immunoblotting. Samples of solubilized proteins prepared as described in the preceding section were resolved by SDS-PAGE (60) in a mini-gel apparatus (Bio-Rad MiniProtean) and transferred electrophoretically (107) to nitrocellulose filters (0.2-μm pore size; Schleicher and Schuell). The protein blots were probed with rabbit polyclonal anti-Sst2, anti-Gpa1, or other antisera (or the mouse 9E10 anti-c-Myc MAb) as the primary antibodies. The resulting immune complexes were detected by incubation with 1:10,000 dilutions of horseradish peroxidase-conjugated goat anti-rabbit or horse anti-mouse immunoglobulin antibodies (Bio-Rad). These secondary antibodies were detected by using a commercial chemiluminescence detection system (ECL; Amersham) in accordance with the incubation and wash conditions recommended by the manufacturer.

To verify expression of epitope-tagged proteins, strain FC180 was transformed with plasmids expressing either the modified (pAB23-*SST2*-myc or pAB23-*GPA1*-myc) or unmodified (pAB23-*SST2* or pAB23-*GPA1*) version of the corresponding gene. Cultures of the transformants were grown to mid-exponential phase in SCGlc, collected by centrifugation, resuspended and lysed directly in 1× SDS-PAGE sample buffer, and examined by immunoblotting with appropriate antibodies as described above.

Cell fractionation by differential solubilization. The abilities of various treatments to solubilize Sst2, Gpa1, and other cellular proteins were examined. These treatments included incubation with (i) six physiochemically distinct detergents, namely, 3-[(3-cholamidopropyl)-dimethyl-ammonio]-1-propanesulfonate (CHAPS), Triton X-100, digitonin, β-octylglucopyranoside, Zwittergent 3-10, and SDS; (ii) a monovalent salt (NaCl); (iii) two divalent cations ($MgCl_2$ and $CaCl_2$); and (iv) two chaotropic agents (urea and Na_2CO_3). In these experiments, cultures of the protease-deficient strain BJ2168 were grown in YPGlc to mid-exponential phase, treated with α-factor (1 μM for 1 h), quenched, harvested by centrifugation, washed twice in buffer B (40 mM triethanolamine hydrochloride [pH 7.2], 2 mM EDTA, 2 mM dithiothreitol, 0.4 mM phenylmethylsulfonyl fluoride), resuspended in the same buffer, transferred to 1.5-ml microcentrifuge tubes, and homogenized with glass beads as described above. The lysate was clarified by centrifugation at 450 × *g* for 20 min. Each of equal portions of the resulting supernatant solution was mixed with an equal volume of one of the following (at the indicated temperature): water (4 and 15°C), 10% CHAPS (4°C), 10% Triton X-100 (4°C), 10% digitonin (4°C), 10% β-octylglucopyranoside (4°C), 10% Zwittergent 3-10 (15°C), 0.5 M NaCl (4°C), 10 mM $MgCl_2$ plus 10 mM $CaCl_2$ (4°C), 0.2 M Na_2CO_3 (15°C), 5 M urea (15°C), or 10% SDS (15°C). After 1 h, the samples were subjected to centrifugation at 100,000 × *g* for 20 min in the TLA 100.3 rotor of a tabletop ultracentrifuge (Beckman TL100) at either 4 or 15°C. The resulting supernatant solution was diluted with an equal volume of 2× SDS-PAGE sample buffer; the pellet was resuspended in twice the original sample volume of 1× SDS-PAGE sample buffer. After being boiled for 10 min, the solubilized samples were resolved by SDS-PAGE in an 8% polyacrylamide gel, transferred electrophoretically to a nitrocellulose filter, and probed with appropriate antibodies.

Cell fractionation by differential centrifugation. Conditions for preparation and lysis of spheroplasts and differential centrifugation were modified from those of Bowser and Novick (17). The cells to be examined (equivalent to an A_{600} of 10) were washed twice with SK (1.2 M sorbitol, 0.1 M KPO_4 [pH 7.5]), resuspended in 1 ml of the same buffer containing 25 mM 2-mercaptoethanol, and incubated with 20 μg of Zymolyase 100T (Kirin Brewery) for 45 min at 30°C. All subsequent manipulations were performed 4°C. The resulting spheroplasts were washed once in SK and resuspended in 2 ml of buffer C (0.8 M sucrose, 20 mM triethanolamine hydrochloride [pH 7.2], 1 mM EDTA, 1 mM dithiothreitol, 0.2 mM phenylmethylsulfonyl fluoride, 10 μg of leupeptin per ml, 10 μg of pepstatin per ml, 10 μg of benzamidine per ml) and disrupted by 20 strokes in a motor-driven Potter-Elvehjem homogenizer. The lysate was cleared of unbroken cells and large debris by centrifugation at 450 × *g* for 20 min and then subjected to centrifugation for 20 min at 10,000 × *g*, yielding a pellet fraction (P1) and a supernatant fraction (S1). S1 was subjected to centrifugation for 20 min at 45,000 × *g*, yielding a second pellet fraction (P2) and a supernatant fraction (S2). S2 was subjected to centrifugation for 20 min at 100,000 × *g*, yielding a final pellet (P3) and supernatant (S3) fraction. S3 and each of the three pellet fractions were adjusted to the same volume and a final concentration with 1× SDS-PAGE sample buffer (or, for the pellet fractions, 1× SDS-PAGE sample buffer containing 4 M urea) and boiled for 10 min (or, for the pellet fractions, heated at 37°C for 20 min). The resulting solubilized samples were resolved by SDS-PAGE, transferred electrophoretically to nitrocellulose filters, and probed with appropriate antisera as described above.

Cell fractionation by sucrose gradient sedimentation. Samples (650 μl) of spheroplast lysates clarified by centrifugation at 450 × *g*, prepared as described in the preceding section, were each mixed gently with 110 μl of 2-(*N*-morpholino)ethanesulfonic acid (MES), pH 6.5, and 610 μg of powdered sucrose (to yield a final sucrose concentration of 70% [wt/vol]). After all of the sucrose was dissolved, each solution was transferred with a wide-mouthed pipette to the bottom of a thin-walled polypropylene tube in the holder of a swinging-bucket rotor (Beckman SW50.1) and carefully overlaid consecutively with 1 ml each of 60, 50, 40, and 30% (wt/vol) sucrose. The samples were then subjected to centrifugation for 16 h at 4°C and 190,000 × *g* in an ultracentrifuge (Beckman L5-50E). Sixteen equal portions (300 μl each) were drawn from each tube, starting at the top, diluted 1:1 with 2× SDS-PAGE sample buffer (or 2× SDS-PAGE sample buffer containing 4 M urea), and boiled at 100°C (or heated at 37°C). The top-most and bottom-most fractions (including the pellet) were discarded, and fractions 2 to 15 were resolved by SDS-PAGE and immunoblotting by the methods described in preceding sections. Undiluted aliquots of each fraction were also analyzed for protein content by using a commercial kit (Bio-Rad Protein Assay System) in accordance with the manufacturer's instructions, and the relative A_{595} generated was recorded for each. The optical diffraction of another undiluted aliquot of each fraction was examined to determine the concentration of sucrose present.

Protein localization by indirect immunofluorescence and confocal microscopy. Labeling and microscopic observation of cells by indirect immunofluorescence were performed essentially as described by Pringle et al. (84), with minor modifications, with strain FC180 or BC159, transformed with plasmid pAB23-*SST2*, pAB23-*SST2*-myc, pAB23-*GPA1*, pAB23-*GPA1*-myc, pBM258, or pBM-KX22, propagated on the appropriate medium to maintain selection for the indicated plasmid, and then shifted to YPGlc for two to four doublings just prior to fixation. pBM258 is YCp50 containing the *GAL1/10* promoter; pBM-KX22 is pBM258 containing the *KEX2* gene (85). Confocal fluorescence microscopy was performed with the assistance of S. Ruzin (Department of Plant Biology, University of California at Berkeley).

Measurement of pheromone response by Ste4 mobility shift. Ste4 (Gβ) phosphorylation upon treatment of *MAT***a** cells with α-factor, and its accompanying shift in electrophoretic mobility (from an M_r of ~49,000 to an M_r of ~56,000), have been described previously (25). Briefly, whole-cell lysates were prepared by resuspending and homogenizing cells directly in SDS-PAGE sample buffer, as described above. The resulting extracts were resolved by SDS-PAGE, transferred to nitrocellulose, and probed with polyclonal anti-Ste4 antisera.

Measurement of pheromone response by halo bioassay for growth arrest. An agar diffusion bioassay (halo assay) to measure response to and recovery from pheromone-induced cell cycle arrest has been described in detail previously (51, 86, 99). Cells from an overnight culture of the strain to be tested were diluted to a final volume of 1.5 ml in an appropriate selective medium. An equal volume of 1.5% (wt/vol) molten agar (50°C) was added, and the suspension was immediately poured into a petri dish already containing the same selective agar medium. Sterile cellulose filter disks (6-mm diameter; Difco) were spotted with appropriate doses of synthetic α-factor and placed with sterile forceps on the top agar containing the nascent lawn, and the plates were incubated for 2 to 5 days at 30°C.

Physical association between Sst2 and a Gpa1-GST fusion. A protease-deficient strain (BJ2168) carrying either pAD4M-GST or pAD4M-*GPA1*-GST was grown at 30°C to mid-exponential phase in SCGlc lacking leucine. Each culture was split into two equal portions and incubated for 90 min in either the absence or the presence of α-factor (5 μM final concentration) to induce Sst2 expression. Alternatively, cultures of an *sst2*-deficient strain (BC180) carrying either pAB23 or pAB23-*SST2* and transformed with either pAD4M-GST or pAD4M-*GPA1*-GST were grown to mid-exponential phase in SCGlc lacking uracil and leucine. Growth was terminated by addition of a final concentration of 10 mM NaN_3 and chilling on ice. Samples (equivalent to 5 × 10^8 cells) of each culture were harvested at 4°C by centrifugation at 2,000 × *g* for 10 min, washed by resuspension and recentrifugation in ice-cold buffer B (40 mM triethanolamine [pH 7.2], 2 mM EDTA, 2 mM dithiothreitol, 0.15 M NaCl, 1 mM AEBSF [4-(2-aminoethyl)-benzenesulfonyl fluoride hydrochloride], and 10 μg each of leupeptin, pepstatin, benzamidine, and aprotinin per ml), resuspended in 500 μl of buffer A containing 50 mM $MgCl_2$ and 10 μM guanosine-5′-*O*-thiotriphosphate (GTPγS) (or 10 μM GDP), and ruptured at 4°C by vortex mixing with glass beads for 4 min total. The resulting lysate was clarified by centrifugation at 2,000 × *g* twice for 10 min each; membranes in the supernatant fraction were solubilized in a final concentration of 1% Triton X-100 and incubated on ice for 1 h. An aliquot (30 μl) of a 1:1 slurry of glutathione-Sepharose 4B beads (Pharmacia) in buffer A was added to the mixture and then incubated on a roller drum in a 4°C room for 2 h. Beads, recovered by brief centrifugation with a microcentrifuge, were washed by resuspension and recentrifugation three times in 20 mM sodium phosphate (pH 7.3) containing 150 mM NaCl and subsequently resuspended in 100 μl of SDS-PAGE sample buffer. Bound proteins were eluted by boiling for 10 min, resolved by SDS-PAGE in either 8 or 12.5% polyacrylamide gels, and analyzed by immunoblotting, as described above, with either anti-Sst2 or anti-GST antibodies.

RESULTS

Specific immunodetection of the *SST2* gene product. To monitor expression of the 698-residue *SST2* gene product, we prepared rabbit polyclonal antibodies directed against a C-terminal segment of the protein (residues 334 to 698). The antiserum was specific for Sst2, because upon SDS-PAGE and immunoblotting of cell extracts, only a single prominent band was detected (Fig. 1A); because this species was absent in cells carrying an *sst2* null mutation and was greatly overproduced in cells harboring a multicopy plasmid expressing the *SST2* gene (Fig. 1A); and because the level of this protein was markedly elevated in *MAT***a** cells treated with α-factor (Fig. 1A) and undetectable in *MAT***a**/*MAT*α cells (data not shown), as reported previously for *SST2* mRNA (27, 30). Also, the mobility of the immunoreactive band with respect to marker proteins of known molecular mass (data not shown) corresponded to a molecular mass of 82 kDa, which is in good agreement with the calculated molecular mass of the Sst2 polypeptide (79.7 kDa) (30).

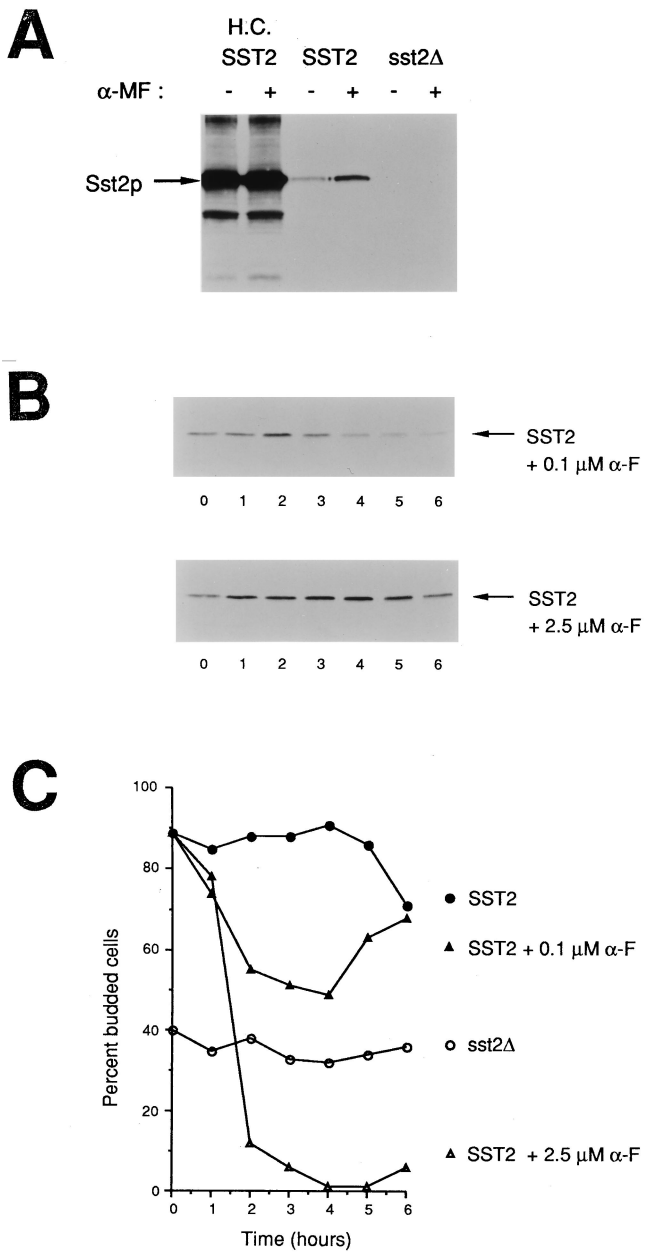

FIG. 1. Immunodetection of Sst2 and kinetics of Sst2 induction. (A) Strain BC159 (*SST2*$^+$) carrying an empty multicopy vector (pAB23) (labeled SST2) and its otherwise isogenic *sst2-Δ2* derivative (BC180) carrying the same vector (pAB23) (labeled sst2Δ) or a derivative of it in which *SST2* was expressed from the constitutive *TDH3* promoter (pAB23-*SST2*) (labeled H.C. SST2) were grown to mid-exponential phase in SCGlc medium lacking leucine and then either not treated (−) or treated with 1 μM (final concentration) α-factor (α-F) (+) for 3 h. Equivalent portions (~10 μg of total protein) of the pellet fractions of cell lysates were resolved by SDS-PAGE, transferred electrophoretically to nitrocellulose filters, and incubated with the rabbit polyclonal anti-Sst2 antiserum, prepared as described in Materials and Methods. Immune complexes were visualized by chemiluminescence. The migration position of Sst2 is indicated. (B) Strains BC159 (SST2) and BC180 (sst2Δ) were grown to mid-exponential phase, divided into equal portions, and either not treated or treated with 0.1 or 2.5 μM α-factor (α-F) over the course of 6 h, as indicated. Samples of the BC159 cultures were removed every hour and examined as described for panel A. (C) Additional aliquots of the samples described for panel B were fixed in formaldehyde (5% final concentration), and the percentage of budded cells present at each time point was determined by direct examination of >200 cells from each sample with a phase-contrast microscope.

Kinetics of induction and disappearance of Sst2 after pheromone treatment. To determine how Sst2 expression is correlated with the process of pheromone-induced cell cycle arrest and the subsequent resumption of growth, immunoblotting was employed to monitor Sst2 levels in *MAT***a** cells treated over the course of several hours with two different concentrations of α-factor (Fig. 1B). At the higher concentration of pheromone (2.5 μM), cells underwent a persistent G_1 arrest, as judged by the accumulation of unbudded cells (Fig. 1C) and, under these conditions, displayed a sustained induction of Sst2. At the lower concentration of pheromone (0.1 μM), resumption of cell cycling began within the time course of the experiment. In this case, the burst of Sst2 synthesis clearly preceded the onset of recovery by at least 2 h. As expected, in *SST2*$^+$ control cells not treated with pheromone, only a low basal level of Sst2 was observed, and in *sst2*Δ control cells, no Sst2 was detectable (data not shown). As has been observed previously for *sst2* point mutants (22), the *sst2*Δ mutants grew somewhat more poorly than otherwise isogenic *SST2*$^+$ cells, as judged by the greater proportion of unbudded cells in the culture (Fig. 1C).

At both concentrations of α-factor tested (Fig. 1B), the level of Sst2 increased following pheromone administration but then declined, despite the continued presence of pheromone, suggesting that Sst2 has a relatively short half-life. To determine whether pheromone treatment affects the rate of Sst2 turnover (as well as its rate of synthesis), *MAT***a** cells were grown to mid-exponential phase, divided into equal subcultures, and treated for 1 h in the absence or presence of 5 μM α-factor to induce Sst2 synthesis. The cells were then collected and exposed to pheromone for an additional hour in the absence or presence of the protein synthesis inhibitor cycloheximide to block further Sst2 synthesis. As determined by immunoblotting (data not shown), the initial 1-h exposure to pheromone led to Sst2 induction and an additional hour of treatment caused a further elevation of Sst2 levels. If cycloheximide was present during the second hour, the level of Sst2 was reduced to the same extent, proportionally, regardless of whether pheromone was present. Thus, α-factor treatment stimulates Sst2 synthesis but not Sst2 degradation. To estimate the rate of Sst2 turnover, a more detailed kinetic analysis of the loss of Sst2 after pheromone induction and treatment with cycloheximide was performed (data not shown). Quantitation of immunoblots by densitometry indicated that the initial half-life was about 30 min. Thus, Sst2 appears to be a rather unstable protein, as expected for a regulatory molecule.

Gpa1 is not required for induction of Sst2. When *GPA1* is nonfunctional or not expressed, haploid cells undergo a persistent G_1 arrest because the Gβγ complex is liberated and constitutively activates the mating response pathway (31, 75). Some evidence suggests that Gα stimulates an adaptation pathway (74). It was formally possible, therefore, that the permanent G_1 arrest observed in Gpa1-deficient cells was due in part to a failure to express Sst2. To address this issue directly, we examined the levels of Sst2 in a pair of otherwise isogenic *GPA1*$^+$ and *gpa1*Δ strains that also carry the *ste5-3*^{ts} mutation (Table 1). At 34°C, the mating signaling pathway is inoperative in *ste5-3*^{ts} cells because of inactivation of Ste5 function (76); therefore, the *gpa1*Δ strain can be propagated. Upon lowering the temperature to 24°C, pheromone response pathway function is restored (because of reactivation of Ste5 protein) and the *gpa1*Δ strain undergoes constitutive G_1 arrest. The *GPA1 ste5-3*^{ts} strain grows normally at both 34 and 24°C. As expected, when the *GPA1 ste5-3*^{ts} cells were grown to mid-exponential phase at 24°C and then either shifted to 34°C or maintained at 24°C for the equivalent of two doublings, little or no Sst2 was detectable (Fig. 2, right); likewise, when the same strain was

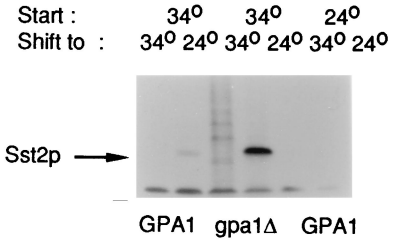

FIG. 2. Activation of the pheromone response pathway via loss of Gpa1 induces Sst2 expression. Strains DJ803-11-1 (*GPA1 ste5-3^{ts}*) (GPA1) and DJ803-2-1 (*gpa1Δ ste5-3^{ts}*) (gpa1Δ) were grown at either 34 or 24°C to mid-exponential phase and then divided into two subcultures, which were shifted to either 34 or 24°C, as indicated. After the equivalent of two doublings, the cells were harvested and lysed, and the whole-cell extracts were resolved by SDS-PAGE and immunoblotting with anti-Sst2 antibodies. The presence of Gpa1 in strain DJ803-11-1 was confirmed by probing the same protein blot with anti-Gpa1 antiserum (data not shown).

grown at 34°C and then shifted to 24°C or maintained at 34°C, little or no Sst2 was produced (Fig. 2, left). In contrast, when *gpa1Δ ste5-3^{ts}* cells were grown at 34°C and then shifted to 24°C, Sst2 was strongly induced, whereas the same cells maintained at 34°C produced no Sst2 (Fig. 2, middle). Therefore, the permanent G_1 arrest observed in *gpa1* mutants was not due to lack of Sst2 expression. A corollary of this finding is that when Gpa1 is absent, Sst2 cannot promote adaptation, which is consistent with the notion that Gpa1 is the target of Sst2 action.

Sst2 has two separate functional domains. To gain insight into how Sst2 may act, we reexamined its deduced primary sequence and searched specifically for homology with known regulators of other transmembrane signaling systems. In such pairwise alignments, statistically significant similarity was found between Sst2 and two families of regulatory proteins (Fig. 3A). First, the N-terminal 300 residues of Sst2 are similar (Fig. 3B) to regions found in two mammalian proteins, bovine GTPase-activating protein (GAP) (108) and human neurofibromatosis tumor suppressor protein (NF-1) (4, 119), and, to a somewhat lesser extent, to regions of other GAP-related proteins, such as *S. cerevisiae* Ira1 and Ira2 (106) (data not shown). Both GAP and NF-1 stimulate in vitro GTP hydrolysis by the low-molecular-weight G-protein p21^{ras} (71, 118). The apparent homology between Sst2 and these other proteins corresponds to part of the segment of GAP that is both necessary and sufficient for its stimulation of p21^{ras} GTPase activity (70).

The second region of similarity is between Sst2 and a recently discovered family of polypeptides, dubbed RGS proteins. The first member, Gos8, was isolated from a human cDNA library and thought to be a transcription factor (117). However, a close relative of Gos8, termed G_α-interacting protein (GAIP), was isolated from a HeLa cell cDNA library via the yeast two-hybrid screen with human $G_{13}\alpha$ as the bait and was able (as a GST fusion) to bind radiolabeled $G_{13}\alpha$ in vitro (29). Additional homologs have been found in *Caenorhabditis elegans* (53) and in mammalian tissues (35, 96). Detailed alignments (29, 35, 53, 96, 117) show that the RGS proteins contain three highly conserved elements, designated Gos8 homology (or GH) domains, and that homologous sequences are present at the C-terminal end of Sst2 (Fig. 3A). In the metazoan proteins, the GH1, GH2, and GH3 domains are immediately juxtaposed to each other, whereas in Sst2, the three GH ele-

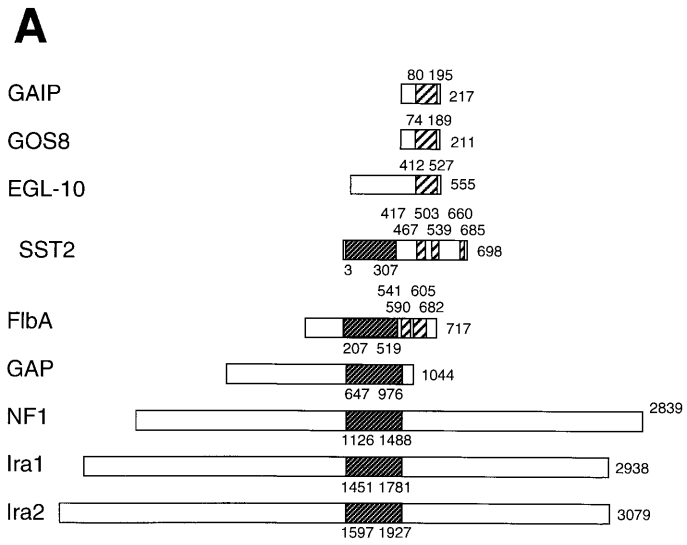

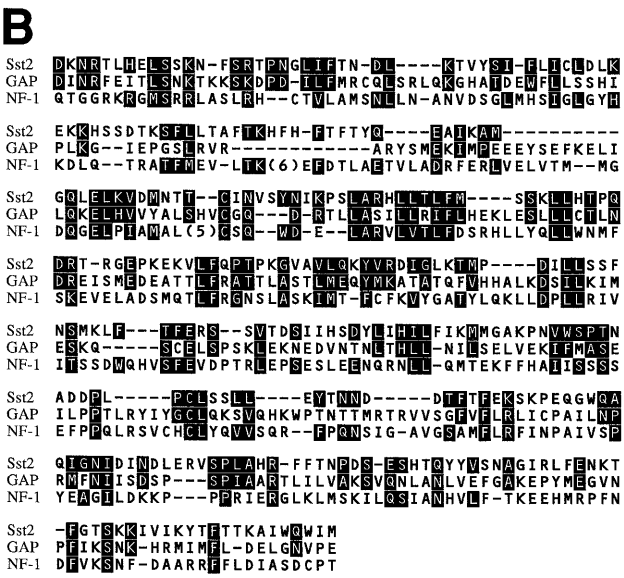

FIG. 3. Sst2 has sequence similarity to both RGS proteins and GTPase-activating proteins. (A) Positions of the GAIP or Gos8 homology (GH) domains of RGS proteins (sparsely hatched boxes) (96) and the GAP homology regions (densely hatched boxes) (4) are shown for human GAIP (29), human Gos8 (117), *C. elegans* EGL-10 (53), *S. cerevisiae* Sst2 (30), *A. nidulans* FlbA (94), human Ras-GAP and neurofibromin (NF-1) (4), and *S. cerevisiae* Ira1 and Ira2 (106). The numbers to the right of the bars indicate the total number of residues. The numbers above the bars indicate the positions of the residues at the N- and C-terminal boundaries of the GH domains. The numbers below the bars indicate the positions of the residues at the N- and C-terminal boundaries of the GAP homology regions. (B) Detailed alignment of the portion of Sst2 that is similar to the known catalytic domains of human GAP (70) and NF-1 (4). Identities and conventional conservative substitutions (K, R, and H; D and E; N and Q; S and T; Y, F, and W; P, G, and A; L, V, I, and M; D and N; and Q and E) (106) shared between Sst2 and either GAP or NF-1 are given as white-on-black letters. Dashes indicate one-residue gaps introduced to optimize the alignment; two larger gaps (in NF-1 only) are given as numbers in parentheses. Alignment of the 305-residue portion of Sst2 and the 330-residue portion of GAP indicated in panel A was generated by the BestFit program, as described in the Wisconsin Package manual, version 8.0 (Genetics Computer Group, Madison, Wis.). Overall similarity for this computer-generated alignment, which introduced 12 gaps, is 42.7% with a quality score of 103 (where the average quality score [± standard deviation] was 95 ± 3 when 50 randomized versions of the Sst2 sequence were compared with GAP), indicating that the similarity detected by this alignment is statistically significant. NF-1 was aligned manually so as to optimize its similarity to both Sst2 and GAP over this same region.

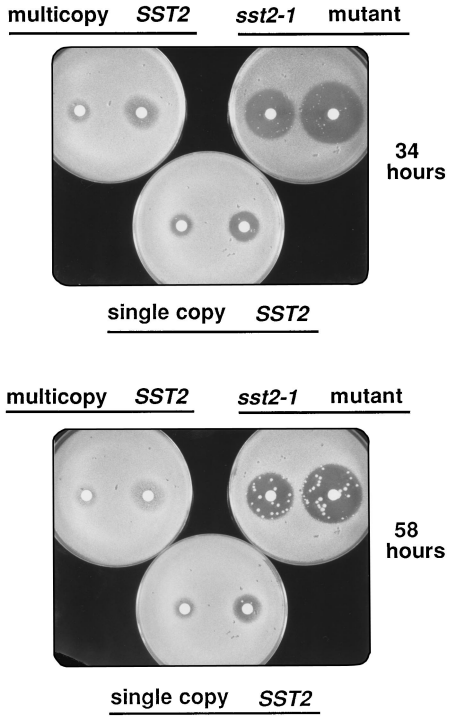

FIG. 4. Overproduction of Sst2 promotes adaptation. Strain RK512-5B (*MAT***a** *sst2-1*) was transformed with either an empty multicopy vector, YEp24 (18) (right), pBC20 (YEp24 carrying the entire *SST2* gene and its promoter) (left), or pBC10 (the entire *SST2* gene and its promoter inserted into YIp5 [104] and integrated in single copy at the *SST2* locus on chromosome 12) (middle), and then a halo bioassay was performed on each transformant at 30°C on SCGlc plates lacking uracil, as described in Materials and Methods, with two doses of α-factor (0.5 and 2 μg [left and right, respectively], for the indicated periods.

ments are separated from each other by spacers of significant length. In currently available databases, the only protein with detectable similarity to Sst2 over both its GAP-like and RGS-like domains is FlbA, a regulator from *Aspergillus nidulans* (62) (Fig. 3A).

The level of Sst2 protein appears to be rate limiting for recovery of cells from pheromone-induced cell cycle arrest, since introduction of the *SST2* gene on a multicopy plasmid not only restores normal pheromone sensitivity to an *sst2* mutant but also accelerates the rate at which growth resumes, as judged by comparing the sizes and turbidities of the halos observed in the standard agar diffusion bioassay (Fig. 4). To determine which regions of Sst2 are required for its function in vivo, we generated a series of N- and C-terminally truncated alleles and then tested whether the truncated proteins retained their recovery-promoting activity. Removal of even a small portion of the N terminus (residues 1 to 55) totally eliminated the biological activity of Sst2 (Fig. 5A), despite the fact that the resulting truncated protein was produced stably in yeast cells at a level equivalent to that of the full-length protein (Fig. 5B). As summarized in Fig. 5C, removal of just 11 residues from the C terminus of Sst2, which does not perturb any of the conserved residues in the RGS-like domain, was tolerated. However, a 141-residue truncation that deleted the GH3 element of the RGS-like domain completely eliminated Sst2 function. Thus, both the GAP-like domain and the RGS-like domain appear to be required for Sst2 function in vivo. In further support of this conclusion, the dominant gain-of-function alleles of Sst2 described previously are due to a single substitution mutation (Pro to Leu) at residue 20 (32), which lies within the GAP-like region (Fig. 3B), and certain loss-of-function *sst2* alleles generated by a random mutagenesis strategy possess only single substitution mutations (Glu to Gly at residue 445 and Tyr to Ser at residue 685), which fall in highly conserved positions within the GH1 and GH3 domains (Fig. 3A), respectively (45a).

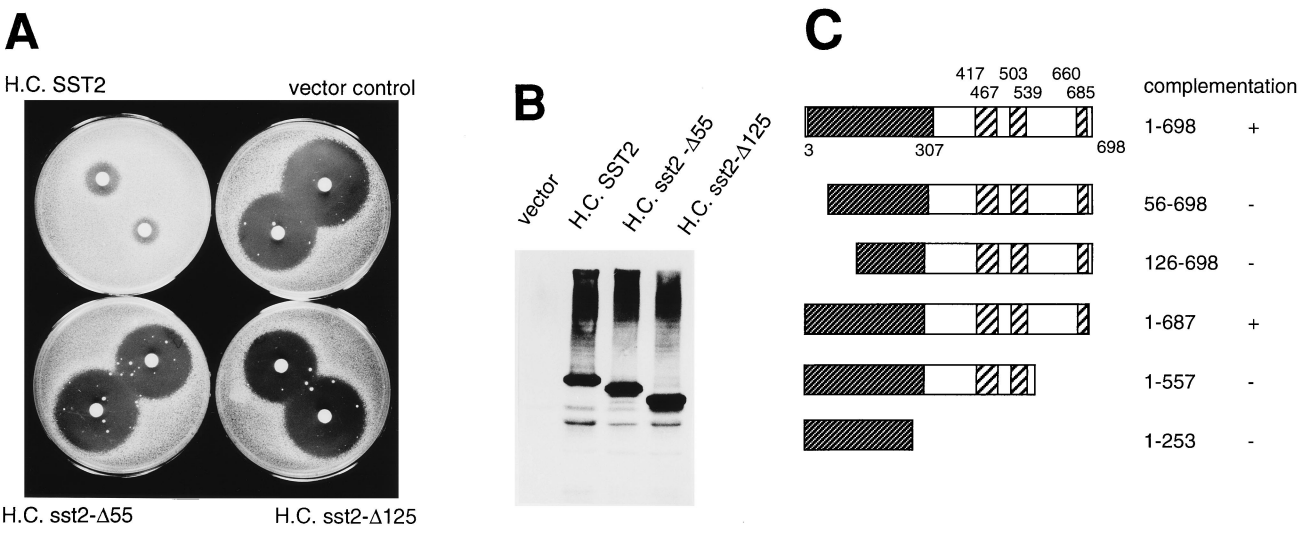

FIG. 5. The N-terminal GAP-like domain and the C-terminal GH domain are both required for Sst2 function. (A) Strain BC180 (*MAT***a** *sst2*Δ) was transformed with an empty multicopy vector (pAD4M) (upper right) or the same vector constitutively expressing from the *ADH1* promoter either normal *SST2* (upper left) or one of two N-terminal truncation mutations, *sst2*(Δ*1–55*) (H.C. sst2-Δ55; lower left) and *sst2*(Δ*1–125*) (H.C. sst2-Δ125; lower right), and then a halo bioassay was performed on each transformant at 30°C on SCGlc plates lacking leucine, as described in Materials and Methods, with two doses of pheromone (1.5 and 5 μg) for 56 h. (B) Expression of Sst2 and the N-terminally truncated derivatives in the cells shown in panel A was confirmed by immunoblotting with anti-Sst2 antibodies, as described in the legend to Fig. 1. (C) Ability of N- and C-terminally truncated Sst2 mutants to complement the hypersensitive phenotype and recovery defect of strain BC180. The three C-terminal truncation mutations shown were constructed as described in Materials and Methods and expressed and tested for function in a manner identical to that described for panel A. GAP and RGS domains are as described in the legend to Fig. 3. +, full complementation (equivalent to *SST2*$^+$); −, no detectable complementation (equivalent to *sst2*Δ).

These observations indicate that Sst2 is a bipartite and perhaps bifunctional protein. These features suggest that Sst2 may exert its negative regulatory effects by binding (via its RGS-like region) directly to Gpa1 and then affecting (via its GAP-like domain) some activity of Gpa1 (possibly its rate of GTP hydrolysis). This model makes several predictions, some of which we were able to test.

Colocalization of Sst2 and Gpa1. If Sst2 promotes adaptation and recovery by deactivating Gpa1, then this regulator and its target should reside in the same subcellular location. A significant fraction of Gpa1 is presumed to be associated with the plasma membrane because it is coupled to pheromone receptors (13, 102), which are mainly present at the cell surface (69). To examine localization of Gpa1 and Sst2, we used differential centrifugation as a preliminary method for subcellular fractionation. The distribution of both proteins, as well as that of marker proteins diagnostic for various organelles and subcellular compartments, was assessed by immunoblotting. Pheromone-treated and control cells were prepared, converted to spheroplasts, and lysed by gentle homogenization, as described in Materials and Methods. The resulting lysates were clarified by low-speed centrifugation to remove unbroken cells and then separated by successively higher-speed centrifugations into four fractions: the pellet (P1) of a 10,000 $\times$ *g* sedimentation, the pellet (P2) of a 45,000 $\times$ *g* sedimentation, the pellet (P3) of a 100,000 $\times$ *g* sedimentation, and the final supernatant fraction (S) of the 100,000 $\times$ *g* sedimentation. The majority of the Gpa1 was found in the P1 fraction, and it was also readily detectable in the P2 and P3 fractions; it was least abundant in the soluble (S) fraction (data not shown). Despite the hydrophilic character of its deduced amino acid sequence (30), Sst2 was also present predominantly in the P1 fraction, was slightly less abundant in the P3 fraction, was present at a somewhat lower level in the P2 fraction, and, except for a degradation product, was least abundant in the soluble (S) fraction (data not shown). Thus, Gpa1 and Sst2 appeared to be largely membrane-associated proteins.

To better characterize the membranes with which Gpa1 and Sst2 are associated, spheroplast lysates were prepared from pheromone-treated and control cells and fractionated by flotation in a sucrose density gradient according to the method of Bowser and Novick (17). This procedure resulted in the formation of a nearly linear gradient of sucrose, and the overall distribution of protein achieved was unaffected by treatment of the cells with pheromone (Fig. 6A). The majority of the Gpa1 (both its 54-kDa myristoylated and 56-kDa unmyristoylated forms) and a large proportion of the Sst2 were found in fractions 10 and 11 and were associated with membranes that collected at a density equivalent to that of ~45% sucrose (Fig. 6B). Sst2 and Gpa1 were also found associated with very dense material near the bottom of the gradient (fractions 14 and 15). Of the seven markers tested, only the α-factor receptor (Ste2), a plasma membrane protein, and Ste4, another component of the receptor-coupled G protein, showed the same specific enrichment in fractions 10 and 11 as Sst2 and Gpa1 (Fig. 6B). The distribution of Atp2 (an integral protein of the mitochondrion) was skewed toward a slightly lighter fraction; this protein was most prominent in fractions 9 and 10 (Fig. 6C). The bulk of the Sec61 (an integral protein of the endoplasmic reticulum membrane) collected at a much lighter density (fractions 4 and 5), equivalent to that of ~33% sucrose (Fig. 6C). Likewise, Sec4 (a peripheral protein of the secretory vesicle, plasma membrane, and Golgi apparatus), although present in every fraction, was most prominent in fractions 4 and 5 (Fig. 6C), in which no Sst2 or Gpa1 was detectable (Fig. 6B). Pgk1 (a cytosolic protein) and Kex2 (an integral protein of the Golgi compartment membrane) were highly enriched in the densest fractions examined (fractions 14 and 15); however, a detectable amount of Kex2 was also observed in fractions 10 and 11 (Fig. 6B). Thus, both Gpa1 and Sst2 were largely plasma membrane-associated proteins (although some Gpa1 and Sst2 seemed to be present in the Golgi compartment and in the soluble fraction). Thus, sucrose buoyant density sedimentation demonstrated that Sst2 and Gpa1 cofractionate, consistent with a functional association.

Immunolocalization of Sst2 and Gpa1. A 16-residue c-Myc epitope was attached to the C terminus in place of the last 10 residues of the Sst2 polypeptide. In Gpa1, a shorter (12-residue) version of the epitope was introduced between residues 126 and 127, a site representing the junction between a domain conserved among all G proteins and a 110-residue insert unique to Gpa1 (81). Each tagged construct complemented a null mutation in the corresponding chromosomal locus and was expressed at a level comparable to that observed for the native protein, as determined by SDS-PAGE and immunoblotting (data not shown). The subcellular distribution of Sst2 and Gpa1 in situ was examined by indirect immunofluorescence microscopy of the epitope-tagged versions. Consistent with its enrichment in the plasma membrane fraction in vitro, Gpa1 stained in patches around the periphery of the cell and in a punctate distribution pattern within the cell; the latter spots were coincident with an authentic Golgi marker (Kex2) when cells were costained with anti-Kex2 antibodies (data not shown). In contrast, Sst2 staining was much more diffuse throughout the cytosol but was excluded from the vacuole and the nucleus (visualized by staining with DAPI [4′,6-diamidino-2-phenylindole]); confocal microscopy of *MAT***a**/*MAT***a** diploid cells confirmed that Sst2 was excluded from the vacuole and nucleus (detected by staining with propidium iodide) and revealed a more granular distribution, with the greatest concentration of Sst2 in punctate bodies at or near the cell surface and near the nucleus, but more abundant and more disperse than the pattern observed for Gpa1 (data not shown). Given the demonstrated instability of Sst2, the diffuse cytosolic staining pattern may represent soluble proteolytic fragments of Sst2-Myc.

Differential solubilization of Sst2 and Gpa1 from membranes. Cofractionation of Gpa1 and Sst2 upon isopycnic banding of membranes in a sucrose gradient and the presence of Sst2 and Gpa1 in the same regions of the cell, as viewed by immunofluorescence microscopy, suggest that these proteins have an opportunity to associate physically. As a prelude to determining whether Sst2 and Gpa1 can bind directly to each other, we established the conditions required for their extraction from membranes. To this end, we examined the ability of various treatments to solubilize Sst2 and Gpa1 from the particulate material prepared from a protease-deficient strain that was grown to mid-exponential phase and treated with pheromone to induce Sst2 expression, as described in Materials and Methods.

Using immunoblotting (data not shown), we found that, for membranes prepared in the presence of Mg^{2+} and Ca^{2+}, virtually all of the Sst2 was found in the pellet. In EDTA-containing buffer, much of the Sst2 remained in the pellet but a significant pool (30 to 40%) was now present in the soluble fraction. In the presence or absence of divalent cations, almost all of the Gpa1 (>90%) remained in the particulate material. Two zwitterionic detergents (CHAPS and Zwittergent 3-10), three nonionic detergents (Triton X-100, digitonin, and octylglucoside), and a strong anionic detergent (SDS) were able to release all or a substantial fraction of the Gpa1 into the soluble fraction, although octylglucoside was the least effective. In

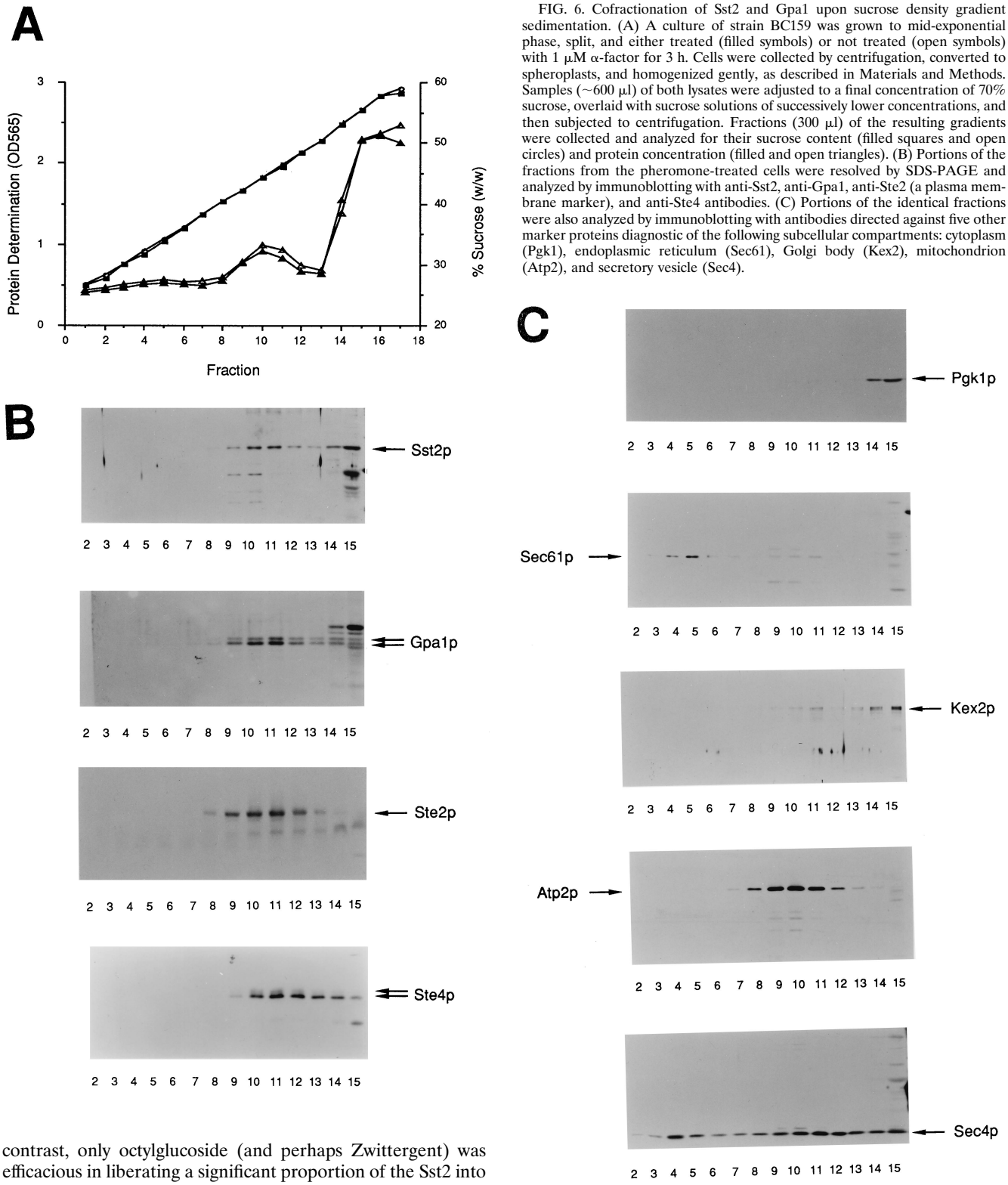

FIG. 6. Cofractionation of Sst2 and Gpa1 upon sucrose density gradient sedimentation. (A) A culture of strain BC159 was grown to mid-exponential phase, split, and either treated (filled symbols) or not treated (open symbols) with 1 μM α-factor for 3 h. Cells were collected by centrifugation, converted to spheroplasts, and homogenized gently, as described in Materials and Methods. Samples (~600 μl) of both lysates were adjusted to a final concentration of 70% sucrose, overlaid with sucrose solutions of successively lower concentrations, and then subjected to centrifugation. Fractions (300 μl) of the resulting gradients were collected and analyzed for their sucrose content (filled squares and open circles) and protein concentration (filled and open triangles). (B) Portions of the fractions from the pheromone-treated cells were resolved by SDS-PAGE and analyzed by immunoblotting with anti-Sst2, anti-Gpa1, anti-Ste2 (a plasma membrane marker), and anti-Ste4 antibodies. (C) Portions of the identical fractions were also analyzed by immunoblotting with antibodies directed against five other marker proteins diagnostic of the following subcellular compartments: cytoplasm (Pgk1), endoplasmic reticulum (Sec61), Golgi body (Kex2), mitochondrion (Atp2), and secretory vesicle (Sec4).

contrast, only octylglucoside (and perhaps Zwittergent) was efficacious in liberating a significant proportion of the Sst2 into the soluble fraction. Conversely, treatment with a high concentration of NaCl, with alkaline sodium carbonate, or with a modest concentration of urea was able to release the majority of the Sst2 into the soluble fraction; however, the same treatments were not effective at extracting Gpa1 into the soluble fraction. On the basis of these findings and other experiments, we formulated an extraction procedure for the simultaneous solubilization of both Gpa1 and Sst2 from the particulate fraction, as described in detail in Materials and Methods.

Sst2 and Gpa1-GST physically interact. To determine if Sst2 physically associates with Gpa1 in vivo, we examined the ability of the two proteins to copurify. As a first approach, we

produced (using the *ADH1* promoter on a multicopy vector) either GST alone or a chimeric protein in which GST was fused to the C terminus of Gpa1 in a protease-deficient (but otherwise wild-type) strain. To induce expression of the chromosomal *SST2* gene, the cells were treated with α-factor. Thereafter, cell lysates were prepared, solubilized, incubated with glutathione-agarose beads in the presence of 50 mM $MgCl_2$ and 10 μM GTPγS, and washed thoroughly, and the bound proteins were analyzed by immunoblotting as described in detail in Materials and Methods. A high Mg^{2+} concentration was used to promote GDP-GTP exchange on Gpa1 (56) and also because this condition reduced nonspecific binding of Sst2 to glutathione-agarose. GTPγS was added to promote G-protein subunit dissociation (52), but similar results were obtained with GDP (data not shown). Under these conditions, a readily detectable amount of Sst2 bound to the beads containing Gpa1-GST (despite potential competition from endogenous Gpa1) whereas none was retained by beads carrying GST alone (Fig. 7A). As expected, Sst2 was retained by the beads only when extracts were prepared from pheromone-treated cells and even though full expression of Sst2 was hindered by overexpression of Gpa1-GST (which significantly reduced the pheromone sensitivity of the cells).

To confirm these findings, either Gpa1-GST or GST alone was overproduced in an *sst2*Δ strain that also carried either an empty vector or the same plasmid overexpressing *SST2* constitutively. Under these conditions, an abundant amount of Sst2 was retained by the Gpa1-GST beads but not by the beads containing GST alone (Fig. 7B), despite the fact that Sst2 was overexpressed to comparable levels in both cases (Fig. 7C). These results suggest that the interaction between Sst2 and Gpa1 is most likely direct and of quite high affinity because the membranes were solubilized and the beads were incubated and washed extensively in both detergent and a high concentration of salt.

Mutations in *GPA1* predicted to reduce the rate of GTP hydrolysis affect adaptation. One potential effect of the association of Sst2 with Gpa1 might be to stimulate the rate at which Gpa1 hydrolyzes bound GTP. If so, cells expressing mutant forms of Gpa1 that are unable to hydrolyze GTP might have a phenotype that resembles that of *sst2* mutants (22, 86). Furthermore, such GTPase-defective Gpa1 proteins might not be susceptible to Sst2 action. To test these predictions, site-directed mutagenesis was used to introduce amino acid replacements into Gpa1 that are known to severely impair the GTPase activity of other Gα subunits. The first mutation, $GPA1^{R297H}$, alters an Arg residue that is conserved in all Gα subunits (81) and is the site of cholera toxin-catalyzed ADP-ribosylation in $G_s\alpha$ and $G_t\alpha$ (19, 109). The second mutation, $GPA1^{Q323L}$, alters a Gln residue that is conserved in all small *ras*-like GTPases (59) and in all Gα subunits (81) and has been shown to be required for the GTPase activity of $G_s\alpha$ (40, 72). In human $G_s\alpha$, equivalent substitutions (R201H and Q227L) are naturally occurring oncogenic mutations (61), suggesting that these alterations cause the active GTP-bound form of $G_s\alpha$ to persist in vivo. Unfortunately, neither $GPA1^{R297H}$ nor $GPA1^{Q323L}$ could complement a *gpa1*Δ mutation, even when overexpressed, suggesting that they too are facilely converted to (or locked in) their activated state and unable to sequester Gβγ effectively. Alternatively, the mutant Gpa1 proteins might be totally misfolded and inactive, thereby preventing their association with Gβγ. Therefore, to test these alternatives, it was necessary to express the GTPase-deficient Gpa1 mutant proteins in $GPA1^{+}$ cells.

Multicopy plasmids expressing normal *GPA1* and each of the mutant proteins from a strong constitutive promoter (*TDH3*), as well as a vector (pAB23) control, were introduced into otherwise isogenic $SST2^{+}$ and *sst2*Δ recipients. The halo bioassay was used to measure response to and subsequent recovery from pheromone. The *sst2*Δ cells (Fig. 8B) were exposed to a 30-fold lower concentration of α-factor than were the $SST2^{+}$ cells (Fig. 8A). High-level expression of normal *GPA1* greatly reduced pheromone response and promoted the resumption of growth in both normal and *sst2*Δ cells (see upper left of each panel in Fig. 8), as has been observed previously (26, 31, 78, 113). If the GTPase-deficient Gpa1 mutants are totally inert, they should have no effect on the response of cells to pheromone; however, if the mutant Gpa1 proteins are still functional but are in a conformational equilibrium that favors the GTP-bound form, then some effect on pheromone response might be expected. Indeed, in $SST2^{+}$ cells expressing $GPA1^{R297H}$, the diameter of the halo observed was distinctly larger than in control cells expressing the vector alone (Fig. 8). This same effect was consistently observed over a range of α-factor concentrations. The most likely explanation for the increased sensitivity is that the mutant Gpa1 molecules in the GTP-bound state are capable of associating with Sst2 but cannot be discharged. By titrating out Sst2 in this manner, Sst2 presumably encounters the endogenous Gpa1 less efficiently, thereby reducing the rate at which the normal Gpa1 molecules are converted back to the GDP-bound state and, thus, capable of recapturing Gβγ. In support of this view, in *sst2* mutant cells expressing $GPA1^{R297H}$, the opposite effect was observed; namely, the diameter of the halo was distinctly smaller than in control cells expressing vector alone (Fig. 8). This result suggests that in the absence of Sst2, the overriding effect of Gpa1(R297H) (at least some of which must be in the GDP-bound state) is to contribute to the total pool of Gpa1 that is competent to reassociate with Gβγ. [High-level expression of the other GTPase-defective mutant, $GPA1^{Q323L}$, in normal cells caused slow growth, suggesting that unlike Gpa1(R297H), Gpa1(Q323L) causes a partially constitutive activation of the pheromone response pathway, most likely because of inefficient coupling to Gβγ (data not shown).]

Sst2 affects short-term response to pheromone. Using the halo bioassay to measure long-term pheromone response and recovery (over the course of days), it is clear that elevated expression of *SST2* (or *GPA1*) accelerates desensitization and promotes recovery (Fig. 4). When Sst2 is produced at a high level (from a constitutive promoter on a multicopy plasmid), cells are all the more refractory to pheromone-induced cell cycle arrest, even at relatively high doses of pheromone (Fig. 5A), presumably because they respond only transiently and adapt very rapidly. If Sst2 stimulates adaptation by converting Gpa1 back to its GDP-bound state, it should be possible to show that the level of Sst2 affects the state of the receptor-coupled G protein immediately following its activation. Others have demonstrated previously that dissociation of Gα from Gβγ upon pheromone administration is accompanied by a rapid phosphorylation of Gβ and that this modification causes a pronounced gel mobility shift, from an M_r of ~49,000 to ~56,000 (25). Hence, Ste4 phosphorylation provides a convenient and reasonably quantitative method to monitor an early event in pheromone response.

*MAT***a** cells were exposed to α-factor, and immediately thereafter, samples of the cultures were withdrawn at various times and analyzed by SDS-PAGE and immunoblotting with anti-Ste4 antibodies. In wild-type ($SST2^{+}$) cells not treated with pheromone, most of the Ste4 was present in its unphosphorylated form (Fig. 9A, middle four lanes). Within 10 min following pheromone addition, the majority of the Ste4 was converted to its phosphorylated form, and by 90 min after

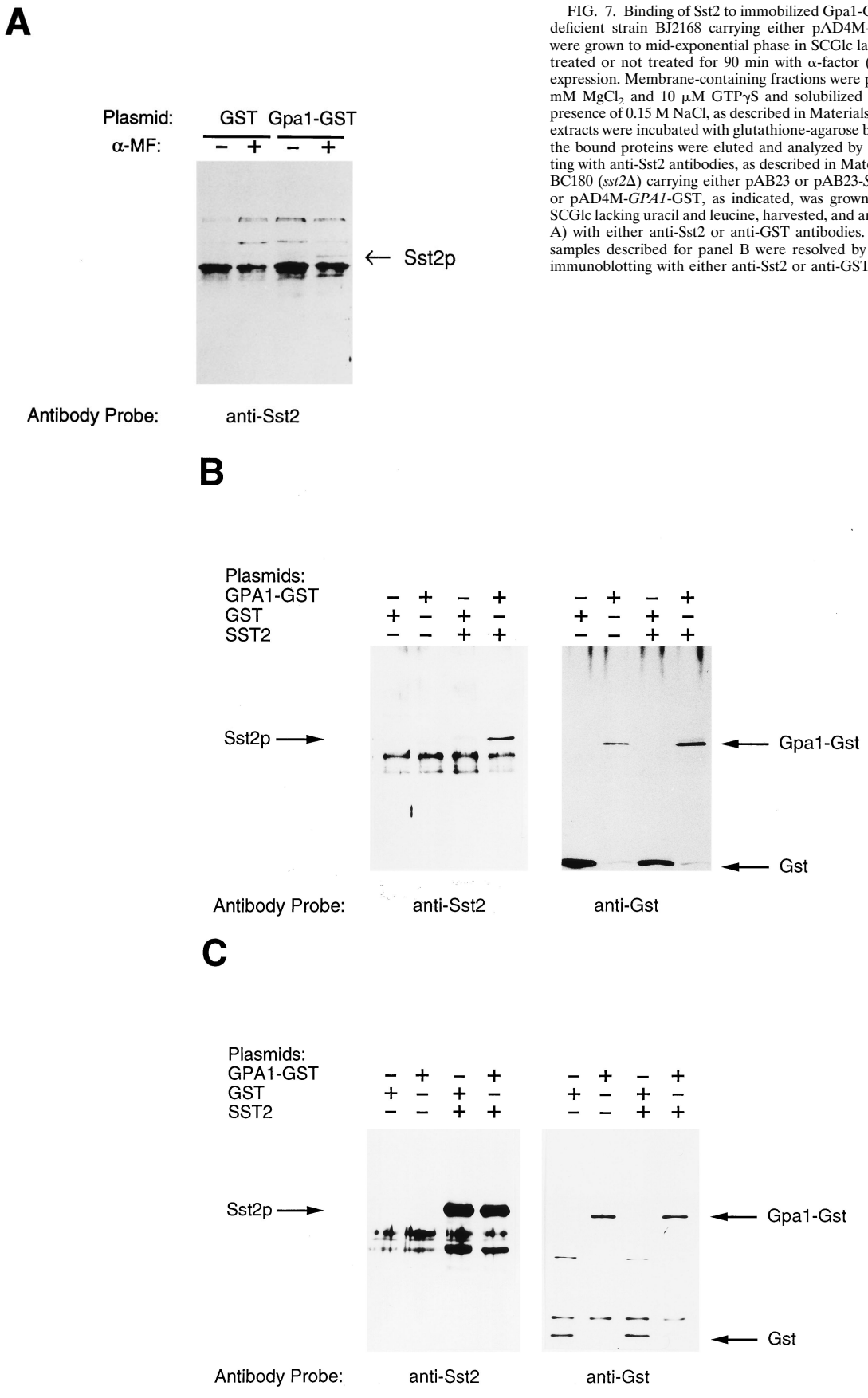

FIG. 7. Binding of Sst2 to immobilized Gpa1-GST. (A) Cultures of protease-deficient strain BJ2168 carrying either pAD4M-GST or pAD4M-*GPA1*-GST were grown to mid-exponential phase in SCGlc lacking leucine, split, and either treated or not treated for 90 min with α-factor (α-MF; 5 μM) to induce Sst2 expression. Membrane-containing fractions were prepared in the presence of 50 mM $MgCl_2$ and 10 μM GTPγS and solubilized with 1% Triton X-100 in the presence of 0.15 M NaCl, as described in Materials and Methods. The solubilized extracts were incubated with glutathione-agarose beads. After extensive washing, the bound proteins were eluted and analyzed by SDS-PAGE and immunoblotting with anti-Sst2 antibodies, as described in Materials and Methods. (B) Strain BC180 (*sst2*Δ) carrying either pAB23 or pAB23-*SST2* and either pAD4M-GST or pAD4M-*GPA1*-GST, as indicated, was grown to mid-exponential phase in SCGlc lacking uracil and leucine, harvested, and analyzed (as described for panel A) with either anti-Sst2 or anti-GST antibodies. (C) Whole-cell lysates of the samples described for panel B were resolved by SDS-PAGE and analyzed by immunoblotting with either anti-Sst2 or anti-GST antibodies.

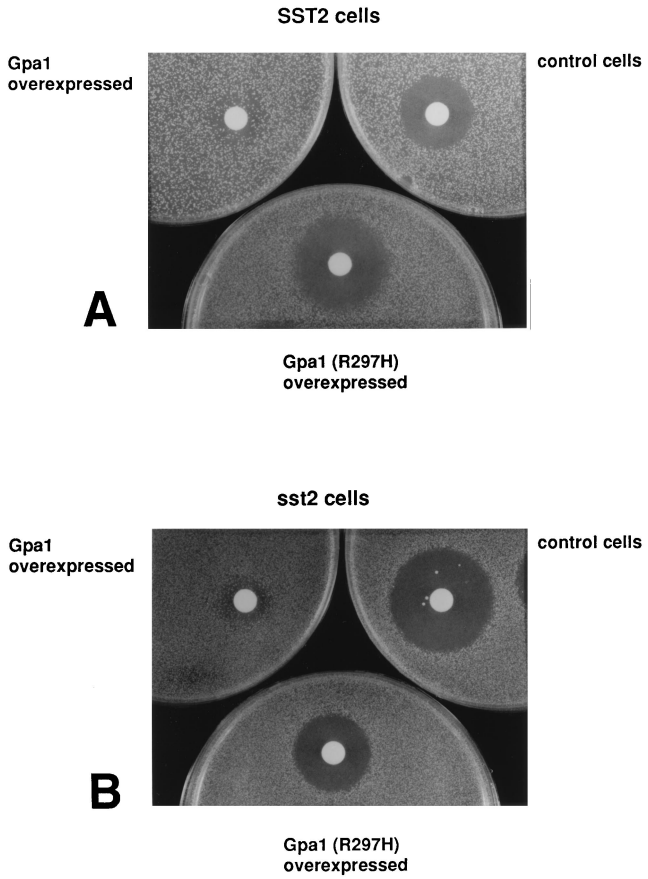

FIG. 8. *GPA1* GTPase-defective mutations affect pheromone response and adaptation. Strain BC159 (SST2 cells) (A) and its otherwise isogenic *sst2*Δ derivative, BC180 (sst2 cells) (B), were transformed with either a high-copy-number vector, pAD4M (control cells; right) or the same vector constitutively expressing from the *ADH1* promoter either normal *GPA1* (Gpa1 overexpressed; left), $GPA1^{R297H}$ [Gpa1(R297H) overexpressed; middle], or $GPA1^{Q323L}$ (not shown), and then a halo bioassay was performed on each transformant at 30°C on SCGlc plates lacking leucine, as described in Materials and Methods, with either 10 μg (upper panel) or 0.3 μg (lower panel) of α-factor for 48 h.

exposure to pheromone, ~90% of the Ste4 was phosphorylated. Strikingly, in *sst2*Δ mutant cells (Fig. 9A, left four lanes), the initial pool of Ste4 already contained a significant level of the phosphorylated form of Ste4, as expected if the absence of Sst2 resulted in a higher steady-state level of GTP-Gpa1 and hence a higher steady-state level of released Gβγ; moreover, in *sst2*Δ cells, a more rapid and nearly quantitative conversion of Ste4 to its phosphorylated form was observed. Conversely, in cells overproducing Sst2 (Fig. 9A, right four lanes), the pool of Ste4 was almost quantitatively in the unphosphorylated state prior to pheromone administration; most significantly, 10 min after pheromone administration, at least 50% of the Ste4 pool still remained in the unphosphorylated state. Even at 90 min after exposure to pheromone a substantial fraction of the Ste4 remained unphosphorylated, as expected if Sst2 facilitates deactivation of Gpa1 and thereby promotes more efficient sequestration of Gβγ.

If the effect of overproduced Sst2 is mediated via an elevated level of deactivated Gpa1, which acts to sequester Gβγ, then overproduction of Gpa1 should similarly impede the pheromone-induced phosphorylation of Ste4. Indeed, compared with wild-type cells (Fig. 9B, left four lanes), the extent of Ste4 phosphorylation was suppressed in cells overproducing Gpa1 (Fig. 9B, middle four lanes), especially at early times (10 and 30 min). In contrast, and as predicted by the model, overexpression of the GTPase-defective $GPA1^{R297H}$ mutant did not significantly reduce the rate or extent of Ste4 phosphorylation after the exposure of cells to pheromone (Fig. 9B, right four lanes).

DISCUSSION

Various genetic and physiological observations suggested previously that Sst2 is a key negative regulator of the pheromone response pathway (21, 22, 86) and that it acts at the level of the receptor or the receptor-coupled G protein (32, 45, 86, 110). The results presented here significantly extend these conclusions by demonstrating that Sst2 negatively regulates pheromone response by direct association with Gpa1 and possibly by stimulating its reconversion to the GDP-bound state, thereby facilitating the recapture of Gβγ.

Despite the hydrophilic character predicted for Sst2 by its primary sequence, a significant fraction of the Sst2 pool was

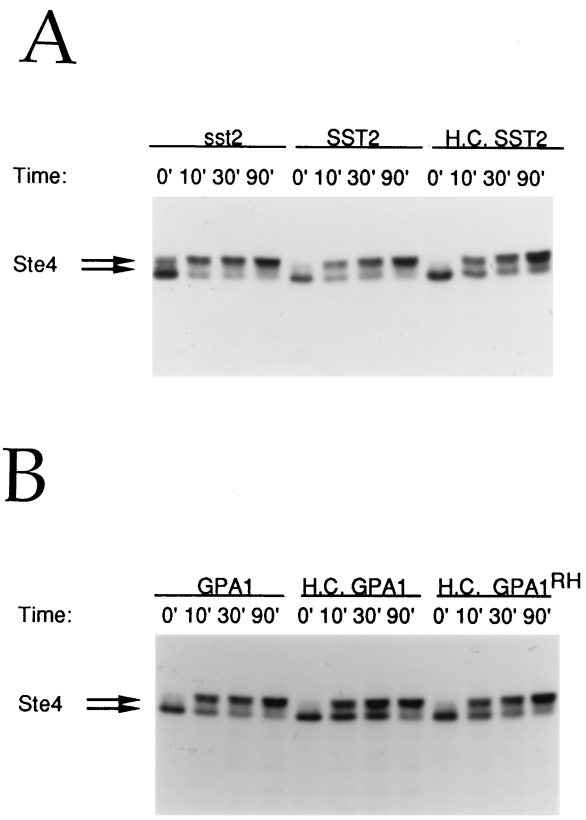

FIG. 9. Sst2 and Gpa1 levels modulate the rate of Ste4 phosphorylation. (A) Strain BC159 transformed either with a multicopy vector, YEp351 (SST2; middle lanes) or with the same vector expressing *SST2* from its own promoter, YEp351-*SST2* (H.C. SST2; right lanes), and strain BC180 (sst2; left lanes) transformed with YEp351 were grown in SCGlc lacking leucine, treated with α-factor (5 μM) for the indicated lengths of time (in minutes), collected by rapid (5-s) centrifugation, resuspended immediately in prewarmed SDS-containing lysis buffer, boiled, and homogenized by glass bead lysis. The resulting whole-cell extracts were resolved by SDS-PAGE and analyzed by immunoblotting with anti-Ste4 antibodies, as described in Materials and Methods. (B) Strain BC159 transformed with a multicopy vector, pAD4M (GPA1; left lanes), or with the same vector constitutively expressing from the *ADH1* promoter either normal *GPA1* (H.C. GPA1; middle lanes) or the GTPase-defective $GPA1^{R297H}$ mutant (H.C. $GPA1^{RH}$; right lanes) was grown, treated with α-factor, and analyzed as described for described panel A.

localized to the plasma membrane and Golgi-derived material, precisely the subcellular fractions in which Gpa1 was most enriched. Association of Sst2 with membranes appeared to be largely via electrostatic interactions, which could be disrupted by altering the pH or the monovalent ion concentration, indicating that Sst2 is a peripheral membrane protein. Association of Gpa1 with membranes appeared to be largely via hydrophobic forces because Gpa1 was only efficiently released from the membrane fraction by detergent treatment. Tight association of Gpa1 with membranes was not unanticipated since Gpa1 is attached to membranes via at least three mechanisms: (i) membrane insertion of its N-terminal myristoyl group (33, 98, 102); (ii) association with the intracellular face of the pheromone receptors, which are polytopic integral membrane proteins (13); and (iii) interaction with Gβγ, which is itself membrane anchored via the C-terminal farnesyl moiety on Gγ (the *STE18* gene product) (111). Consistent with the weaker association of Sst2 with membranes in vitro, indirect immunofluorescence showed that a portion of the Sst2 pool was cytosolic whereas Gpa1 localization was restricted to the plasma membrane and to the Golgi body, which is in agreement with the in vitro fractionation results.

The finding that a significant proportion of the Gpa1 pool localized to the Golgi complex was somewhat surprising. Appearance of Gpa1 in intracellular Golgi-associated vesicles could represent subunits in transit either to or from the plasma membrane. However, there is growing evidence in animal cells for a secondary role of heterotrimeric G proteins in regulating intracellular membrane trafficking events (83, 116). If Gpa1 has such a function, the observed association of some Sst2 with Golgi material raises the possibility that Sst2 also regulates the non-signal-transducing function(s) of Gpa1. Restriction of the expression of both *GPA1* and *SST2* to *MAT***a** and *MAT*α cells further suggests that any role for Gpa1 (and its regulation by Sst2) in membrane trafficking involves a process unique to haploid cells. Gpa1 may have a role in the anisotropic cell growth (projection formation) required for mating that is distinct from its role as a receptor-coupled signal transducer (97a).

We found that haploid cells possess low levels of Sst2 in the absence of pheromone treatment and that synthesis of this protein is markedly induced (at least 10-fold) in response to pheromone. Other RGS proteins are also induced by extracellular stimuli (117). Induction of Sst2 occurs concomitantly with the imposition of G_1 arrest. In the continuous presence of pheromone, the level of Sst2 remains relatively high and declines slowly during the period when cells begin to recover from arrest and resume cell cycling. In the absence of a persistent inductive signal, however, Sst2 disappears relatively rapidly, indicating that the protein is subject to rather rapid proteolytic degradation. These results suggest that the buildup of Sst2 is part of a feedback loop that commences with transcriptional induction of the *SST2* gene in response to the initial events of pheromone response and functions to counteract activation of Gpa1. The dramatic elevation of Sst2 in response to pheromone induction of its transcript is in marked contrast to the situation observed for Gpa1. Although *GPA1* mRNA is induced about fivefold in pheromone-treated cells (49), the total amount of Gpa1 protein does not change detectably upon pheromone induction (although the proportion of myristoylated Gpa1 does increase) (33). Thus, during the pheromone response, the ratio of Sst2 to Gpa1 increases sharply, presumably promoting Sst2-Gpa1 interaction. Thus, regulation of Gpa1 might result simply from the change in Sst2 level. Gpa1 modulation by Sst2 presumably ensures that a full-blown mating response does not ensue unless the number of occupied receptors and the resultant extent of Gβγ dissociation from Gα is sufficiently high and sustained to generate a potent signal.

Once cells have adapted and resumed growth, there is no longer any need for Sst2; in fact, persistence of Sst2 would interfere with the ability of haploid cells to respond to another pheromone challenge. These considerations perhaps explain the physiological advantage of the relatively rapid turnover of Sst2. Positions 544 to 581 and 606 to 626 in Sst2 are especially rich in Pro, Glu (and Asp), Ser, and Thr residues; such PEST motifs are found preferentially in eukaryotic proteins that display rapid turnover (87, 89). These sequences lie precisely within the spacer region that separates the GH2 and GH3 motifs in the C-terminal portion of Sst2 that is homologous to other members of the RGS protein family. Cleavage at these PEST sites would remove the GH3 element, which we showed by deletion analysis to be required for Sst2 function in vivo.

An RGS domain alone is sufficient to mediate RGS protein-Gα subunit interaction, for example, the binding of human GAIP to human $G_{i3}\alpha$ (29). Likewise, the C-terminal RGS-like domain of Sst2 probably mediates its physical association with Gpa1, a supposition we are attempting to test directly in vitro. Our observation that the N-terminal domain of Sst2 resembles a subclass of GTPase-activating proteins suggests a testable model for the mechanism by which Sst2 binding to Gpa1 could promote adaptation. Although some Gα subunits, like $G_s\alpha$, have an intrinsically high rate of GTP hydrolysis (68), other Gα subunits have a very low intrinsic GTPase activity and are markedly stimulated by association with additional protein factors. For example, the GTPase activities of the α subunits of both mammalian Gq (a Gα that binds and activates phospholipase Cβ) (7) and transducin (a Gα that binds and activates retinal cyclic GMP phosphodiesterase) (2) are greatly stimulated when these Gα proteins associate with their targets. It is unlikely that Sst2 is itself an effector for downstream signaling by Gpa1 because *sst2* mutants are mating competent and because little Sst2 exists in cells prior to their exposure to pheromone. Our findings that Gpa1 is not required for Sst2 induction yet Sst2 production in the absence of Gpa1 does not lead to recovery provide evidence that Sst2 must exert it function through Gpa1. Hence, the most parsimonious model for Sst2 action is that it binds directly to Gpa1, stimulates GTP hydrolysis, and thus promotes Gpa1 deactivation. Indeed, we demonstrated that Sst2 is able to associate with a Gpa1-GST fusion in vivo. Likewise, preliminary results indicate that Gpa1 is able to associate with a GST-Sst2 fusion (106a). However, formation of the Sst2-Gpa1-GST complexes was not detectably affected by the nature of the bound nucleotide (GDP versus GTPγS), whereas it might be anticipated that a GAP-like protein would associate tightly only with GTP-bound target. On the other hand, it is possible that the major binding energy for the interaction of Sst2 with Gpa1 is contributed by the C-terminal RGS domain and not by the N-terminal GAP-like region.

In support of the view that Sst2 is able to associate with Gpa1 in its GTP-bound state, we observed that expression of a GTPase-defective mutant of Gpa1 in otherwise normal cells increased their apparent sensitivity to pheromone, suggesting that the mutant Gpa1 molecules interfered with the ability of Sst2 to act on the normal Gpa1 molecules present. In further support of this conclusion, expression of the GTPase-defective Gpa1 mutant protein in cells lacking Sst2 did not increase pheromone sensitivity but rather had the converse effect. Also, our demonstration that elevated levels of either Sst2 or Gpa1 had the similar effect of impeding the release of Gβγ supports the conclusion that Sst2 helps maintain Gpa1 in its inactive

GDP-bound state. Correspondingly, in *sst2*Δ mutants, a significant fraction of Ste4 was already in the phosphorylated state in the absence of pheromone. Moreover, *sst2*Δ mutants grew more slowly than *SST2*$^+$ cells, and a higher proportion of the *sst2*Δ cells were in the unbudded state. These observations indicate that the pheromone signaling pathway is partially activated in Sst2-deficient cells, suggesting that even the basal level of Sst2 likely has a significant role in suppressing signaling that arises from spontaneous dissociation of the receptor-coupled G protein.

Taken together, our findings indicate that Sst2 action impinges on Gpa1 function. By contrast, the C-terminal tail of the α-factor receptor (Ste2) also appears to play some role in adaptation, but various lines of evidence suggest that the receptor and Sst2 contribute to adaptation by two independent mechanisms (55, 86). Although the results presented here are consistent with a role for Sst2 in enhancing the ability of Gpa1 to down-regulate the pheromone response pathway, it is possible that the converse might be true. In other words, association of Sst2 with Gpa1 might be necessary to deliver this regulator to its proper target. From this perspective, one possibility is that the GAP-like domain of Sst2 (like that of mammalian GAP itself) may act on a small G protein. In fact, propagation of the mating signal involves activation of the small Ras-like GTPase Cdc42 (97, 121), which (like Gpa1) is tethered to the plasma membrane (124). Thus, docking of Sst2 to Gpa1 via its RGS domain might bring the GAP-like domain of Sst2 into close juxtaposition to Cdc42, allowing Sst2 to stimulate GTP hydrolysis by Cdc42, thus causing its deactivation. On the other hand, GTPase-activating proteins specific for Cdc42 have been characterized genetically and biochemically in yeast cells (82, 122) and do not bear significant sequence similarity to Sst2 (123). Another possibility, given the similarity of the N terminus of Sst2 to GAP and NF-1 per se, is that association of Sst2 with Gpa1 brings it into close proximity to Ras1 and/or Ras2, which are (like Gpa1 and Cdc42) tethered to the plasma membrane (8). Previous reports have suggested that mating pheromone action interdicts Ras-based signaling, on the basis of pheromone-imposed inhibition of glucose-stimulated cAMP synthesis (which depends on Ras function) (1, 80). However, no direct or indirect role for Ras in the mating signal transduction pathway has yet been uncovered.

As shown here, both the N-terminal GAP-like region and the C-terminal RGS domain of Sst2 are required for its function in vivo. Direct in vitro tests of the hypothesis that Sst2 binding stimulates the GTP hydrolysis activity of Gpa1 and, if so, the determination of whether that effect is specific to Gpa1 and requires its GAP-like domain await purification of amounts of functional forms of both Sst2 and Gpa1 sufficient for biochemical studies.

ACKNOWLEDGMENTS

The studies described here were carried out initially at the University of California at Berkeley with support from postdoctoral fellowship 61-831 from the Jane Coffin Childs Memorial Fund for Medical Research (to H.G.D.), from postdoctoral fellowship J46-89 from the California Division of the American Cancer Society (to D.M.), from postdoctoral fellowship DRG-836 from the Cancer Research Fund of the Damon Runyon-Walter Winchell Foundation (to W.E.C.), and from NIH research grant GM21841 (to J.T.) and then continued at Yale University with support from the Yale-Lederle Cooperative Agreement and research grants from the Donaghue Medical Research Foundation and the American Heart Association (to H.G.D.). This work was also supported by the facilities and staff of the Cancer Research Laboratory of the University of California at Berkeley.

We thank Anne Marie Quinn for advice with regard to evaluating the statistical significance of sequence alignments.

REFERENCES

1. **Arkinstall, S. J., S. G. Papasavvas, and M. A. Payton.** 1991. Yeast α-mating factor receptor-linked G-protein signal transduction suppresses Ras-dependent activity. FEBS Lett. **284:**123–128.
2. **Arshavsky, V., and M. D. Bownds.** 1992. Regulation of deactivation of photo-receptor G protein by its target enzyme and cGMP. Nature (London) **357:**416–417.
3. **Ausubel, F. M., R. Brent, R. E. Kingston, D. D. Moore, J. G. Seidman, J. A. Smith, and K. Struhl (ed.).** 1987. Current protocols in molecular biology. Wiley-Interscience, New York.
4. **Ballester, R., D. Marchuk, M. Boguski, A. Saulino, R. Letcher, M. Wigler, and F. Collins.** 1990. The NFI locus encodes a protein functionally related to mammalian GAP and yeast IRA proteins. Cell **63:**851–859.
5. **Bardwell, L., J. G. Cook, C. J. Inouye, and J. Thorner.** 1994. Signal propagation and regulation in the mating pheromone response pathway of the yeast *Saccharomyces cerevisiae*. Dev. Biol. **166:**363–379.
6. **Baum, P., J. Thorner, and L. Honig.** 1978. Identification of tubulin from the yeast *S. cerevisiae*. Proc. Natl. Acad. Sci. USA **75:**4962–4966.
7. **Berstein, G., J. L. Blank, D. Y. Jhon, J. H. Exton, S. G. Rhee, and E. M. Ross.** 1992. Phospholipase C-β1 is a GTPase-activating protein for Gq/11, its physiologic regulator. Cell **70:**411–418.
8. **Bhattacharya, S., L. Chen, J. R. Broach, and S. Powers.** 1995. Ras membrane targeting is essential for glucose signaling but not for viability in yeast. Proc. Natl. Acad. Sci. USA **92:**2984–2988.
9. **Blinder, D., S. Bouvier, and D. D. Jenness.** 1989. Constitutive mutants in the yeast pheromone response: ordered function of the gene products. Cell **56:**479–486.
10. **Blinder, D., and D. D. Jenness.** 1989. Regulation of postreceptor signaling in the pheromone response pathway of *Saccharomyces cerevisiae*. Mol. Cell. Biol. **9:**3720–3726.
11. **Blumer, K. J., J. E. Reneke, W. E. Courchesne, and J. Thorner.** 1988. Functional domains of a peptide hormone receptor: the α-factor receptor (*STE2* gene product) of the yeast *Saccharomyces cerevisiae*. Cold Spring Harbor Symp. Quant. Biol. **53:**591–603.
12. **Blumer, K. J., J. E. Reneke, and J. Thorner.** 1988. The *STE2* gene product is the ligand-binding component of the α-factor receptor of *Saccharomyces cerevisiae*. J. Biol. Chem. **263:**10836–10842.
13. **Blumer, K. J., and J. Thorner.** 1990. Beta and gamma subunits of a yeast guanine nucleotide-binding protein are not essential for membrane association of the alpha subunit but are required for receptor coupling. Proc. Natl. Acad. Sci. USA **87:**4363–4367.
14. **Blumer, K. J., and J. Thorner.** 1991. Receptor-G protein signaling in yeast. Annu. Rev. Physiol. **53:**37–57.
15. **Boeke, J. D., J. Trueheart, G. Natsoulis, and G. R. Fink.** 1987. 5′-Fluoroorotic acid as a selective agent in yeast molecular genetics. Methods Enzymol. **152:**164–175.
16. **Bourne, H. R., D. A. Sanders, and F. McCormick.** 1991. The GTPase superfamily: conserved structure and molecular mechanism. Nature (London) **127:**117–127.
17. **Bowser, R., and P. Novick.** 1991. Sec15 protein, an essential component of the exocytotic apparatus, is associated with the plasma membrane and with a soluble 19.5S particle. J. Cell Biol. **112:**1117–1131.
18. **Carlson, M., and D. Botstein.** 1982. Two differentially regulated mRNAs with different 5′ ends encode secreted and intracellular forms of yeast invertase. Cell **28:**145–154.
19. **Cassel, D., F. Eckstein, M. Lowe, and Z. Selinger.** 1979. Determination of the turn-off reaction for the hormone-activated adenylate cyclase. J. Biol. Chem. **254:**9835–9838.
20. **Chan, R. K., L. M. Melnick, L. C. Blair, and J. Thorner.** 1983. Extracellular suppression allows mating by pheromone-deficient sterile mutants of *Saccharomyces cerevisiae*. J. Bacteriol. **155:**903–906.
21. **Chan, R. K., and C. A. Otte.** 1982. Isolation and genetic analysis of *Saccharomyces cerevisiae* mutants supersensitive to G1 arrest by **a**-factor and α-factor pheromones. Mol. Cell. Biol. **2:**11–20.
22. **Chan, R. K., and C. A. Otte.** 1982. Physiological characterization of *Saccharomyces cerevisiae* mutants supersensitive to G1 arrest by **a**-factor and α-factor pheromones. Mol. Cell. Biol. **2:**21–29.
23. **Chen, W. J., and M. G. Douglas.** 1987. The role of protein structure in the mitochondrial import pathway. Analysis of the soluble F1-ATPase β-subunit precursor. J. Biol. Chem. **262:**15598–15604.
24. **Ciejek, E., and J. Thorner.** 1979. Recovery of *S. cerevisiae* **a** cells from G1 arrest by α factor pheromone requires endopeptidase action. Cell **18:**623–635.
25. **Cole, G. M., and S. I. Reed.** 1991. Pheromone-induced phosphorylation of a G protein β subunit in *S. cerevisiae* is associated with an adaptive response to mating pheromone. Cell **64:**703–716.
26. **Cole, G. M., D. E. Stone, and S. I. Reed.** 1990. Stoichiometry of G protein subunits affects the *Saccharomyces cerevisiae* mating pheromone signal transduction pathway. Mol. Cell. Biol. **10:**510–517.

27. **Courchesne, W. E., R. Kunisawa, and J. Thorner.** 1986. Control of pheromone response in *Saccharomyces cerevisiae*: isolation of the *SST2* gene. Yeast **2:**S74.
28. **Courchesne, W. E., R. Kunisawa, and J. Thorner.** 1989. A putative protein kinase overcomes pheromone-induced arrest of cell cycling in *S. cerevisiae*. Cell **58:**1107–1119.
29. **De Vries, L., M. Mousli, A. Wurmser, and M. G. Farquhar.** 1995. GAIP, a protein that specifically interacts with the trimeric protein Gαi3, is a member of a protein family with a highly conserved core domain. Proc. Natl. Acad. Sci. USA **92:**11916–11920.
30. **Dietzel, C., and J. Kurjan.** 1987. Pheromonal regulation and sequence of the *Saccharomyces cerevisiae SST2* gene: a model for desensitization to pheromone. Mol. Cell. Biol. **7:**4169–4177.
31. **Dietzel, C., and J. Kurjan.** 1987. The yeast *SCG1* gene: a Gα-like protein implicated in the **a**- and α-factor response pathway. Cell **50:**1001–1010.
32. **Dohlman, H. G., D. Apaniesk, Y. Chen, J. Song, and D. Nusskern.** 1995. Inhibition of G-protein signaling by dominant gain-of-function mutations in Sst2p, a pheromone desensitization factor in *Saccharomyces cerevisiae*. Mol. Cell. Biol. **15:**3635–3643.
33. **Dohlman, H. G., P. Goldsmith, A. M. Spiegel, and J. Thorner.** 1993. Pheromone action regulates G-protein α subunit myristoylation in the yeast *Saccharomyces cerevisiae*. Proc. Natl. Acad. Sci. USA **90:**9688–9692.
34. **Dohlman, H. G., J. Thorner, M. G. Caron, and R. J. Lefkowitz.** 1991. Model systems for the study of seven-transmembrane-segment receptors. Annu. Rev. Biochem. **60:**653–688.
35. **Druey, K. M., K. J. Blumer, V. H. Kang, and J. H. Kehrl.** 1996. Inhibition of G protein-mediated MAP kinase activation by members of a novel mammalian gene family. Nature (London) **379:**742–746.
36. **Evan, G. I., G. K. Lewis, G. Ramsay, and J. M. Bishop.** 1985. Isolation of monoclonal antibodies specific for human c-*myc* proto-oncogene product. Mol. Cell. Biol. **5:**3610–3616.
37. **Fuller, R. S., A. Brake, and J. Thorner.** 1989. Yeast prohormone processing enzyme (*KEX2* gene product) is a Ca^{2+}-dependent serine protease. Proc. Natl. Acad. Sci. USA **86:**1434–1438.
38. **Fuller, R. S., A. J. Brake, and J. Thorner.** 1989. Intracellular targeting and structural conservation of a prohormone-processing endoprotease. Science **246:**482–486.
39. **Gould, B., A. Salminen, N. C. Walworth, and P. J. Novick.** 1988. A GTP-binding protein required for secretion rapidly associates with secretory vesicles and the plasma membrane in yeast. Cell **53:**753–768.
40. **Graziano, M. P., and A. G. Gilman.** 1989. Synthesis in *Escherichia coli* of GTPase-deficient mutants of Gs alpha. J. Biol. Chem. **264:**15475–15482.
41. **Guthrie, C., and G. R. Fink.** 1991. Guide to yeast genetics and molecular biology. Academic Press, Inc., San Diego, Calif.
42. **Harlow, E., and D. Lane.** 1988. Antibodies: a laboratory manual. Cold Spring Harbor Laboratory Press, Cold Spring Harbor, N.Y.
43. **Hartwell, L. H.** 1980. Mutants of *Saccharomyces cerevisiae* unresponsive to cell division control by polypeptide mating hormone. J. Cell Biol. **85:**811–822.
44. **Hasson, M. S.** 1992. Analysis of *Saccharomyces cerevisiae* pheromone response: biochemical and genetic characterization of the Ste5 protein. Ph.D. thesis. University of California, Berkeley.
45. **Hasson, M. S., D. Blinder, J. Thorner, and D. D. Jenness.** 1994. Mutational activation of the *STE5* gene product bypasses the requirement for G protein β and γ subunits in the yeast pheromone response pathway. Mol. Cell. Biol. **14:**1054–1065.

45a. **Hendricks, K. B., and J. Thorner.** Unpublished results.

46. **Herskowitz, I.** 1995. MAP kinase pathways in yeast: for mating and more. Cell **80:**187–197.
47. **Hill, J. E., A. M. Myers, T. J. Koerner, and A. Tzagaloff.** 1986. Yeast/*E. coli* shuttle vectors. Yeast **2:**163–167.
48. **Ito, H., Y. Fukuda, K. Murata, and A. Kimura.** 1983. Transformation of intact yeast cells treated with alkali cations. J. Bacteriol. **153:**163–168.
49. **Jahng, K.-Y., J. Ferguson, and S. I. Reed.** 1988. Mutations in a gene encoding the α subunit of a *Saccharomyces cerevisiae* G protein indicate a role in mating pheromone signaling. Mol. Cell. Biol. **8:**2484–2493.
50. **Jones, E.** 1991. Tackling the protease problem in *Saccharomyces cerevisiae*. Methods Enzymol. **194:**428–453.
51. **Julius, D., L. Blair, A. Brake, G. Sprague, and J. Thorner.** 1983. Yeast α-factor is processed from a larger precursor polypeptide: the essential role of a membrane-bound dipeptidyl aminopeptidase. Cell **32:**839–852.
52. **Kleuss, C., A. S. Raw, E. Lee, S. R. Sprang, and A. G. Gilman.** 1994. Mechanism of GTP hydrolysis by G-protein alpha subunits. Proc. Natl. Acad. Sci. USA **91:**9828–9831.
53. **Koelle, M. R., and H. R. Horvitz.** 1996. EGL-10 regulates G protein signaling in the *C. elegans* nervous system and shares a conserved domain with many mammalian proteins. Cell **84:**115–125.
54. **Koerner, T. J., J. E. Hill, A. M. Myers, and A. Tzagoloff.** 1991. High-expression vectors with multiple cloning sites for construction of *trpE* fusion genes: pATH vectors. Methods Enzymol. **194:**477–490.
55. **Konopka, J. B., D. D. Jenness, and L. H. Hartwell.** 1988. The C-terminus of the *S. cerevisiae* α-pheromone receptor mediates an adaptive response to pheromone. Cell **54:**609–620.
56. **Kozasa, T., and A. G. Gilman.** 1995. Purification of recombinant G proteins from Sf9 cells by hexahistidine tagging of associated subunits. Characterization of alpha-12 and inhibition of adenylyl cyclase by alpha-z. J. Biol. Chem. **270:**1734–1741.
57. **Kurjan, J.** 1993. The pheromone response pathway in *Saccharomyces cerevisiae*. Annu. Rev. Genet. **27:**147–179.
58. **Kurjan, J., J. P. Hirsch, and C. Dietzel.** 1991. Mutations in the guanine nucleotide-binding domains of a yeast Gα protein confer a constitutive or uninducible state to the pheromone response pathway. Genes Dev. **5:**475–483.
59. **Lacal, J. C., and F. McCormick.** 1993. The ras superfamily of GTPases. CRC Press, Inc., Boca Raton, Fla.
60. **Laemmli, U. K.** 1970. Cleavage of structural proteins during the assembly of the head of bacteriophage T4. Nature (London) **227:**680–685.
61. **Landis, C. A., S. B. Masters, A. Spada, A. M. Pace, H. R. Bourne, and L. Vallar.** 1989. GTPase inhibiting mutations activate the α chain of Gs and stimulate adenylyl cyclase in human pituitary tumours. Nature (London) **340:**692–696.
62. **Lee, B. N., and T. H. Adams.** 1994. Overexpression of flbA, an early regulator of *Aspergillus* asexual sporulation, leads to activation of brlA and premature initiation of development. Mol. Microbiol. **14:**323–334.
63. **Levin, D. E., and B. Errede.** 1995. The proliferation of MAP kinase signaling pathways in yeast. Curr. Opin. Cell Biol. **7:**197–202.
64. **Lohse, M. J.** 1993. Molecular mechanisms of membrane receptor desensitization. Biochim. Biophys. Acta **1179:**171–188.
65. **MacKay, V. L., J. Armstrong, C. Yip, S. Welch, K. Walker, S. Osborne, P. Sheppard, and J. Forstrom.** 1991. Characterization of the Bar proteinase, an extracellular enzyme from the yeast *Saccharomyces cerevisiae*. Adv. Exp. Med. Biol. **306:**161–172.
66. **MacKay, V. L., S. K. Welch, M. Y. Insley, T. R. Manney, J. Holly, G. C. Saari, and M. L. Parker.** 1988. The *Saccharomyces cerevisiae BAR1* gene encodes an exported protein with homology to pepsin. Proc. Natl. Acad. Sci. USA **85:**55–59.
67. **Madura, K., and A. Varshavsky.** 1994. Degradation of G alpha by the N-end rule pathway. Science **265:**1454–1458.
68. **Markby, D. W., R. Onrust, and H. R. Bourne.** 1993. Separate GTP binding and GTPase activating domains of a G alpha subunit. Science **262:**1895–1901.
69. **Marsh, L., and I. Herskowitz.** 1988. From membrane to nucleus: the pathway of signal transduction in yeast and its genetic control. Cold Spring Harbor Symp. Quant. Biol. **53:**557–566.
70. **Marshall, M. S., W. S. Hill, S. N. Assunta, U. S. Vogel, M. D. Schaber, E. M. Scolnick, R. A. F. Dixon, I. S. Sigal, and J. B. Gibbs.** 1989. A C-terminal domain of GAP is sufficient to stimulate ras p21 GTPase activity. EMBO J. **8:**1105–1110.
71. **Martin, G. A., D. Viskochil, G. Bollag, P. C. McCabe, W. J. Crosier, H. Haubruck, L. Conroy, R. Clark, P. O'Connell, R. M. Cawthon, et al.** 1990. The GAP-related domain of the neurofibromatosis type 1 gene product interacts with ras p21. Cell **63:**843–849.
72. **Masters, S. B., R. T. Miller, M. H. Chi, F. H. Chang, B. Beiderman, N. G. Lopez, and H. R. Bourne.** 1989. Mutations in the GTP-binding site of Gs alpha alter stimulation of adenylyl cyclase. J. Biol. Chem. **264:**15467–15474.
73. **Milligan, G.** 1993. Agonist regulation of cellular G protein levels and distribution: mechanisms and functional implications. Trends. Pharmacol. Sci. **14:**413–418.
74. **Miyajima, I., K.-I. Arai, and K. Matsumoto.** 1989. $GPA1^{VAL\text{-}50}$ mutation in the mating-factor signaling pathway in *Saccharomyces cerevisiae*. Mol. Cell. Biol. **9:**2289–2297.
75. **Miyajima, I., M. Nakafuku, N. Nakayama, C. Brenner, A. Miyajima, K. Kaibuchi, K. I. Arai, Y. Kaziro, and K. Matsumoto.** 1987. *GPA1*, a haploid-specific essential gene, encodes a yeast homolog of mammalian G protein which may be involved in the mating factor-mediated signal transduction pathway. Cell **50:**1011–1019.
76. **Miyajima, I., N. Nakayama, M. Nakafuku, Y. Kaziro, K. Arai, and K. Matsumoto.** 1988. Suppressors of a gpa1 mutation cause sterility in *Saccharomyces cerevisiae*. Genetics **119:**797–804.
77. **Moore, S. A.** 1984. Yeast cells recover from mating pheromone α-factor-induced division arrest by desensitization in the absence of α-factor destruction. J. Biol. Chem. **259:**1004–1010.
78. **Nomoto, S., N. Nakayama, K. Arai, and K. Matsumoto.** 1990. Regulation of the yeast pheromone response pathway by G protein subunits. EMBO J. **9:**691–696.
79. **Oehlen, B., and F. R. Cross.** 1994. Signal transduction in the budding yeast, *Saccharomyces cerevisiae*. Curr. Opin. Cell Biol. **6:**836–841.
80. **Papasavvas, S., S. Arkinstall, J. Reid, and M. Payton.** 1992. Yeast alpha-mating factor receptor and G-protein-linked adenylyl cyclase inhibition requires RAS2 and GPA2 activities. Biochem. Biophys. Res. Commun. **184:**1378–1385.
81. **Pennington, S. R.** 1994. GTP-binding proteins: heterotrimeric G proteins,

p. 169–356. In P. Sheterline (ed.), Protein profiles, Vol. 1. Academic Press, Ltd., London.
82. **Peterson, J., Y. Zheng, L. Bender, A. Myers, R. Cerione, and A. Bender.** 1994. Interactions between the bud emergence proteins Bem1p and Bem2p and Rho-type GTPases in yeast. J. Cell Biol. **127:**1395–1406.
83. **Pimplikar, S. W., and K. Simons.** 1993. Regulation of apical transport in epithelial cells by a Gs class of heterotrimeric G protein. Nature (London) **362:**456–458.
84. **Pringle, J. R., A. E. M. Adams, D. G. Drubin, and B. K. Haarer.** 1991. Immunofluorescence methods for yeast. Methods Enzymol. **194:**565–602.
85. **Redding, K., C. Holcomb, and R. S. Fuller.** 1991. Immunolocalization of Kex2 protease identifies a putative late Golgi compartment in the yeast *Saccharomyces cerevisiae*. J. Cell Biol. **113:**527–538.
86. **Reneke, J. E., K. J. Blumer, W. E. Courchesne, and J. Thorner.** 1988. The carboxy-terminal segment of the yeast α-factor receptor is a regulatory domain. Cell **55:**221–234.
87. **Rogers, S., R. Wells, and M. Rechsteiner.** 1986. Amino acid sequences common to rapidly degraded proteins: the PEST hypothesis. Science **234:** 364–368.
88. **Roush, W.** 1996. Regulating G protein signaling. Science **271:**1056–1058.
89. **Salama, S. R., K. B. Hendricks, and J. Thorner.** 1994. G_1 cyclin degradation: the PEST motif of yeast Cln2 is necessary, but not sufficient, for rapid protein turnover. Mol. Cell. Biol. **14:**7953–7966.
90. **Sambrook, J., E. F. Fritsch, and T. Maniatis.** 1989. Molecular cloning: a laboratory manual, 2nd ed. Cold Spring Harbor Laboratory Press, Cold Spring Harbor, N.Y.
91. **Sanger, F., S. Nicklen, and A. R. Coulson.** 1977. DNA sequencing with chain-terminating inhibitors. Proc. Natl. Acad. Sci. USA **74:**5463–5467.
92. **Schandel, K. A., and D. D. Jenness.** 1994. Direct evidence for ligand-induced internalization of the yeast α-factor pheromone receptor. Mol. Cell. Biol. **14:**7245–7255.
93. **Scherer, S., and R. W. Davis.** 1979. Replacement of chromosome segments with altered DNA sequences constructed *in vitro*. Proc. Natl. Acad. Sci. USA **76:**4951–4955.
94. **Schultz, J., B. Ferguson, and G. F. Sprague, Jr.** 1995. Signal transduction and growth control in yeast. Curr. Opin. Genet. Dev. **5:**31–37.
95. **Sherman, F., G. R. Fink, and J. A. Hicks.** 1986. Laboratory course manual for methods in yeast genetics. Cold Spring Harbor Laboratory Press, Cold Spring Harbor, N.Y.
96. **Siderovski, D. P., A. Hessel, S. Chung, T. M. Mak, and M. Tyers.** 1996. A new family of G protein-coupled receptor regulators? Curr. Biol. **6:**211–212.
97. **Simon, M. N., C. De Virgilio, B. Souza, J. R. Pringle, A. Abo, and S. I. Reed.** 1995. Role for the Rho-family GTPase Cdc42 in yeast mating-pheromone signal pathway. Nature (London) **376:**702–705.
97a. **Song, J., K. Gunn, and H. G. Dohlman.** 1995. Regulation of cell membrane polarity by a heterotrimeric G protein, p. 272. *In* Abstracts of the Yeast Cell Biology Meeting. Cold Spring Harbor Laboratory, Cold Spring Harbor, N.Y.
98. **Song, J., J. Hirschman, K. Gunn, and H. G. Dohlman.** Regulation of membrane and subunit interactions by N-myristoylation of a G protein α subunit in yeast. J. Biol. Chem., in press.
99. **Sprague, G. F., Jr.** 1991. Assay of yeast mating reaction. Methods Enzymol. **194:**21–37.
100. **Sprague, G. F., Jr., and J. Thorner.** 1992. Pheromone response and signal transduction during the mating process of *Saccharomyces cerevisiae*, p. 657–744. *In* J. R. Broach, J. R. Pringle, and E. W. Jones (ed.), The molecular and cellular biology of the yeast *Saccharomyces*. Cold Spring Harbor Laboratory Press, Cold Spring Harbor, N.Y.
101. **Stirling, C. J., J. Rothblatt, M. Hosobuchi, R. Deshaies, and R. Schekman.** 1992. Protein translocation mutants defective in the insertion of integral membrane proteins into the endoplasmic reticulum. Mol. Biol. Cell. **3:**129–142.
102. **Stone, D. E., G. M. Cole, M. de Barros Lopes, M. Goebl, and S. I. Reed.** 1991. N-Myristoylation is required for function of the pheromone-responsive Gα protein of yeast: conditional activation of the pheromone response by a temperature-sensitive N-myristoyl transferase. Genes Dev. **5:**1969–1981.
103. **Stone, D. E., and S. I. Reed.** 1990. G protein mutations that alter the pheromone response in *Saccharomyces cerevisiae*. Mol. Cell. Biol. **10:**4439–4446.
104. **Struhl, K., D. Stinchcomb, S. Scherer, and R. W. Davis.** 1979. High frequency transformation of yeast: autonomous replication of hybrid DNA molecules. Proc. Natl. Acad. Sci. USA **76:**1035–1039.
105. **Tan, P. K., N. G. Davis, G. F. Sprague, Jr., and G. S. Payne.** 1993. Clathrin facilitates the internalization of seven transmembrane segment receptors for mating pheromones in yeast. J. Cell Biol. **123:**1707–1716.
106. **Tanaka, K., M. Nakafuku, T. Satoh, M. S. Marshall, J. S. Gibb, K. Matsumoto, Y. Kaziro, and A. Toh-e.** 1990. *S. cerevisiae* genes *IRA1* and *IRA2* encode proteins that may be functionally equivalent to mammalian ras GTPase-activating protein. Cell **60:**803–807.
106a. **Tongaonkar, P., and K. Madura.** Personal communication.
107. **Towbin, H., T. Staehelin, and J. Gordon.** 1979. Electrophoretic transfer of proteins from polyacrylamide gels to nitrocellulose sheets: procedure and some applications. Proc. Natl. Acad. Sci. USA **76:**4350–4354.
108. **Trahey, M., G. Wong, R. Halenbeck, B. Rubinfeld, G. A. Martin, M. Ladner, C. M. Long, W. J. Crosier, K. Watt, and K. Koths.** 1988. Molecular cloning of two types of GAP complementary DNA from human placenta. Science **242:**1697–1700.
109. **Van Dop, C., M. Tsubokawa, H. R. Bourne, and J. Ramachandran.** 1984. Amino acid sequence of retinal transducin at the site ADP-ribosylated by cholera toxin. J. Biol. Chem. **259:**696–698.
110. **Weiner, J. L., C. Guttieriez-Steil, and K. J. Blumer.** 1993. Disruption of receptor-G protein coupling in yeast promotes the function of an SST2-dependent adaptation pathway. J. Biol. Chem. **268:**8070–8077.
111. **Whiteway, M., K. L. Clark, E. Leberer, D. Dignard, and D. Y. Thomas.** 1994. Genetic identification of residues involved in association of α and β G-protein subunits. Mol. Cell. Biol. **14:**3223–3229.
112. **Whiteway, M., L. Hougan, D. Dignard, D. Y. Thomas, L. Bell, G. C. Saari, F. J. Grant, P. O'Hara, and V. L. MacKay.** 1989. The *STE4* and *STE18* genes of yeast encode potential β and γ subunits of the mating factor receptor-coupled G protein. Cell **56:**467–477.
113. **Whiteway, M., L. Hougan, and D. Y. Thomas.** 1988. Expression of MFα1 in *MAT***a** cells supersensitive to α-factor leads to self arrest. Mol. Gen. Genet. **214:**85–88.
114. **Whiteway, M., L. Hougan, and D. Y. Thomas.** 1990. Overexpression of the *STE4* gene leads to mating response in haploid *Saccharomyces cerevisiae*. Mol. Cell. Biol. **10:**217–222.
115. **Whiteway, M., and D. Y. Thomas.** 1994. Site-directed mutations altering the CAAX box of Ste18, the yeast pheromone-response pathway Gγ subunit. Genetics **137:**967–976.
116. **Wilson, B. S., M. Komuro, and M. G. Farquhar.** 1994. Cellular variations in heterotrimeric G protein localization and expression in rat pituitary. Endocrinology **134:**233–244.
117. **Wu, H.-K., H. H. Q. Heng, X.-M. Shi, D. R. Forsdyke, L.-C. Tsui, T. W. Mak, M. D. Minden, and D. P. Siderovski.** 1995. Differential expression of a basic helix-loop-helix phosphoprotein gene, *GOS8*, in acute leukemia and localization to human chromosome 1q31. Leukemia **9:**1291–1298.
118. **Xu, G. F., B. Lin, K. Tanaka, D. Dunn, D. Wood, R. Gesteland, R. White, R. Weiss, and F. Tamanoi.** 1990. The catalytic domain of the neurofibromatosis type 1 gene product stimulates ras GTPase and complements *ira* mutants of *S. cerevisiae*. Cell **63:**843–849.
119. **Xu, G. F., P. O'Connell, D. Viskochil, R. Cawthon, M. Robertson, M. Culver, D. Dunn, J. Stevens, R. Gesteland, and R. White.** 1990. The neurofibromatosis type 1 gene encodes a protein related to GAP. Cell **62:**599–608.
120. **Yanisch-Perron, C., J. Vieira, and J. Messing.** 1985. Improved M13 phage cloning vectors and host strains: nucleotide sequences of the M13mp18 and pUC19 vectors. Gene **33:**103–119.
121. **Zhao, Z.-S., T. Leung, E. Manser, and L. Lim.** 1995. Pheromone signalling in *Saccharomyces cerevisiae* requires the small GTP-binding protein Cdc42p and its activator *CDC24*. Mol. Cell. Biol. **15:**5246–5257.
122. **Zheng, Y., R. Cerione, and A. Bender.** 1994. Control of the yeast bud-site assembly GTPase Cdc42. Catalysis of guanine nucleotide exchange by Cdc24 and stimulation of GTPase activity by Bem3. J. Biol. Chem. **269:** 2369–2372.
123. **Zheng, Y., M. J. Hart, K. Shinjo, T. Evans, A. Bender, and R. A. Cerione.** 1993. Biochemical comparisons of the *Saccharomyces cerevisiae* Bem2 and Bem3 proteins. Delineation of a limit Cdc42 GTPase-activating protein domain. J. Biol. Chem. **268:**24629–24634.
124. **Ziman, M., D. Preuss, J. Mulholland, J. M. O'Brien, D. M. Botstein, and D. I. Johnson.** 1993. Subcellular localization of Cdc42p, a *Saccharomyces cerevisiae* GTP-binding protein involved in the control of cell polarity. Mol. Biol. Cell **4:**1307–1316.